Impact of injection rate ramp-up on nucleation and arrest of dynamic fault slip

F. Ciardo[1], A. P. Rinaldi[1], B. Lecampion[2]

[1] *Swiss Seismological Service (SED) at ETH Zürich – Switzerland*

[2] *Geo-Energy Laboratory – Gaznat chair on Geo-Energy – EPF Lausanne - Switzerland*

Modelling and Simulation Forum – UTAH FORGE
15/12/2021

Schweizerischer Erdbebendienst
Service Sismologique Suisse
Servizio Sismico Svizzero
Swiss Seismological Service

ETH zürich

Outline

1. A fast boundary element based solver for localized inelastic deformations
    - Elasticity
    - Constitutive relations for Displacement Discontinuities
    - Solution of the tangent system
    - Preconditioner
    - Few examples
2. Impact of injection rate ramp-up on nucleation and arrest of dynamic fault slip
    - Motivations
    - Fault model
    - Scaling analysis
    - Small Scale Yielding
    - Numerical investigation of the parametric space
    - Model limitations

- Conclusions

[Ciardo F. et al (2020), A fast boundary element based solver for localized inelastic deformations, *Int. J. Numer. Methods Eng., 121, 5696-5718*]

[Ciardo F. & A. P. Rinaldi (2021), Impact of injection rate ramp-up on nucleation and arrest of dynamic fault slip, *Accepted to Geomechanics and Geophysics for Geo-Energy and Geo-Resources (GGGG-D-21-00202R1)*]

A fast boundary element based solver for localized inelastic deformations

Motivations

- Many geo-mechanical applications exhibit localized failures in large domains
    - Faulting
    - Shear-banding
    - Fracturing
- Fast, accurate and mesh independent!
- Boundary Element Method to properly resolve localization phenomena
- No volume integrals but inelastic deformations can only be localized along displacement discontinuity segments (defined a-priori)

Uni-axial compression test

[Taken from Wikipedia]

RETAINING STRUCTURES

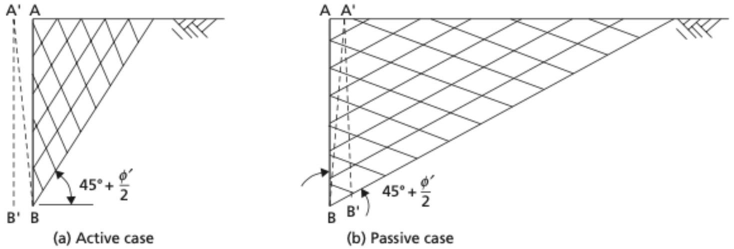

Figure 11.13 Minimum deformation conditions to mobilise: (a) active state, (b) passive state.

[Taken from Knappet J.A. and Craig, R.F., Craig's soil mechanics Book]

BEARING CAPACITY OF SHALLOW FOOTINGS

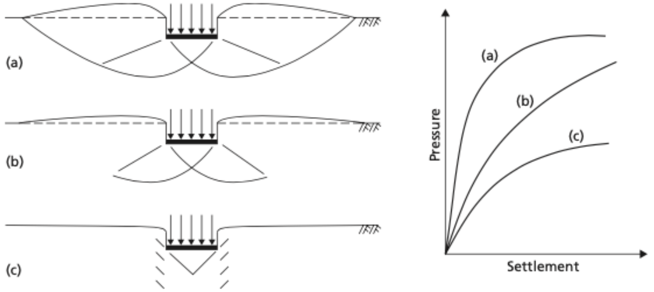

Figure 8.2 Modes of failure: (a) general shear, (b) local shear, and (c) punching shear.

Elasticity

- Plane strain condition
- Infinite or finite domain
- Homogeneous, isotropic and linear elastic
- Impermeable medium

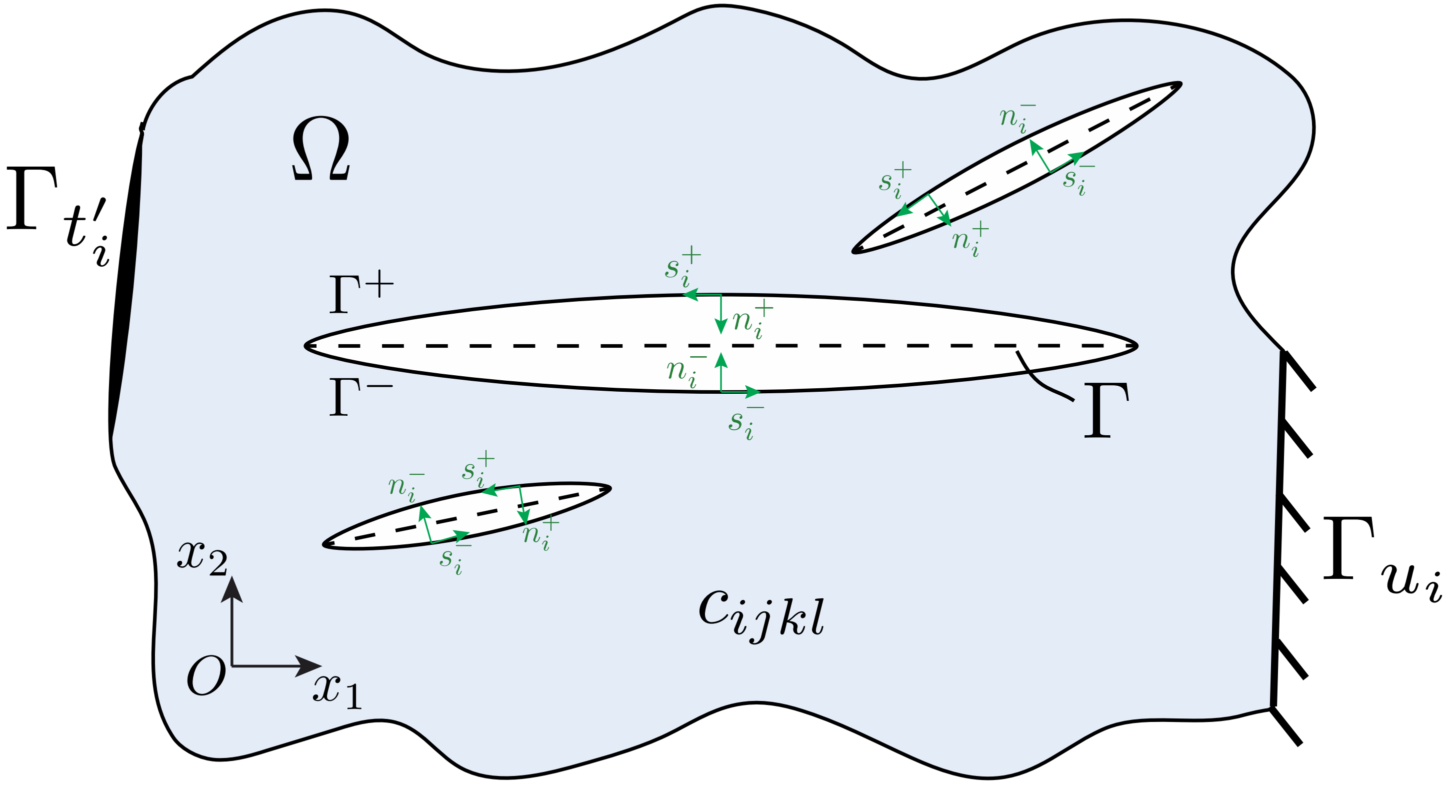

Boundary integral elasticity equations (quasi-static formulation):

$$t_i(\mathbf{x}) - t_i^o(\mathbf{x}) = n_j(\mathbf{x}) \int_\Gamma c_{ijkl} \frac{\partial S_{ab}^k}{\partial \xi_l}(\mathbf{x}, \xi) d_a(\xi) n_b(\xi) \mathrm{d}\xi \quad \text{for} \quad i, j, = n, s$$

$$t_i = \sigma_{ij} n_j \qquad d_i = u_i^+ - u_i^-$$

Constitutive relations for DD segments

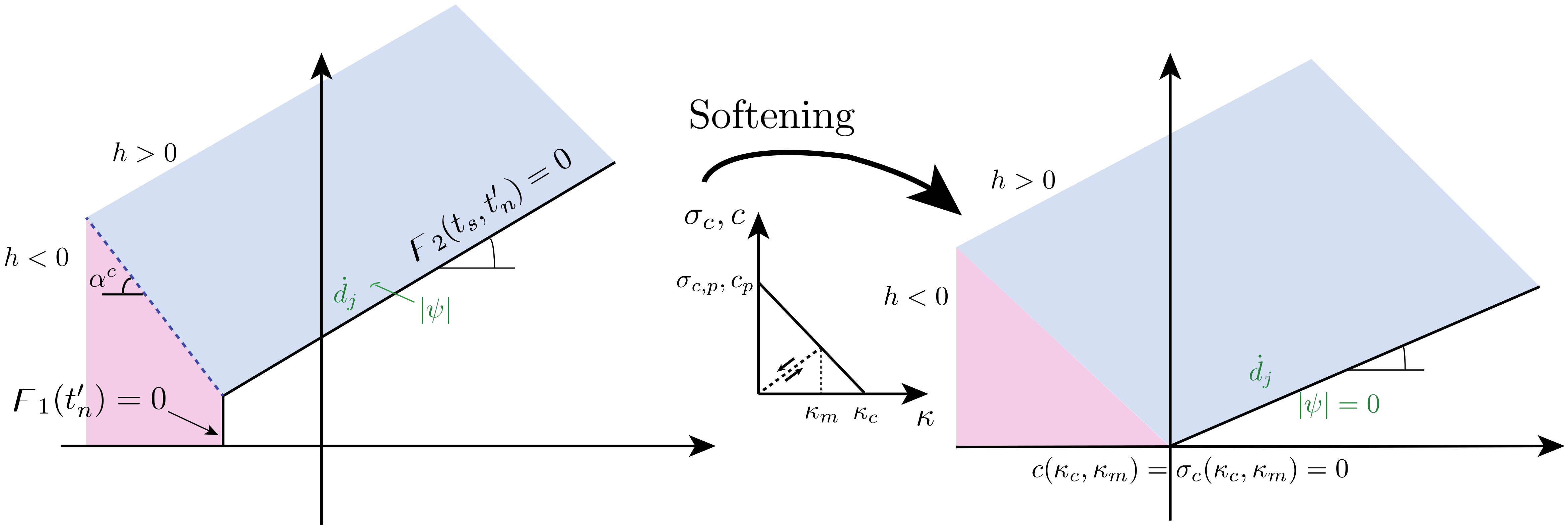

$$F_1(t'_n) = -\sigma_c(\kappa, \kappa_m) - t'_n \leq 0,$$
$$F_2(t_s, t'_n) = |t_s| - c(\kappa, \kappa_m) - f(|d_s|, \delta_m)t'_m \leq 0$$

Initial and boundary conditions

- We assume static equilibrium conditions with initial stress tensor, resulting in tractions t_i^o on Γ

- Localized inelastic deformations therefore occurs as a result of either external loading or via internal pore fluid pressurization *p* which modifies the effective traction on the potential failure segments

$$t_i'(\mathbf{x},t) = t_i^g(\mathbf{x},t) - p(\mathbf{x},t) \qquad \text{on} \qquad \Gamma_{t_i'}$$

$$u_i(\mathbf{x},t) = u_i^g(\mathbf{x},t) \qquad \text{on} \qquad \Gamma_{u_i}$$

$$\Gamma = \Gamma_{u_i} \cup \Gamma_{t_i'}, \text{ and } \Gamma_{u_i} \cap \Gamma_{t_i'} = \emptyset$$

Numerical scheme

- Elasticity ⟶ Displacement Discontinuity Method
  - Piecewise linear approximation
    - No continuity at each intersecting mesh node
    - Good accuracy even with non-uniform meshes

- Hierarchical matrix representation of the BEM combined with adaptive cross approximation
  - Speed up algebraic operations
  - Reduce memory requirements

- Fluid flow ⟶ Finite Volume Method
  - Linear and continuous approximation
  - Node centered FV scheme
    - Intrinsic local mass conservation
    - No need of structured mesh

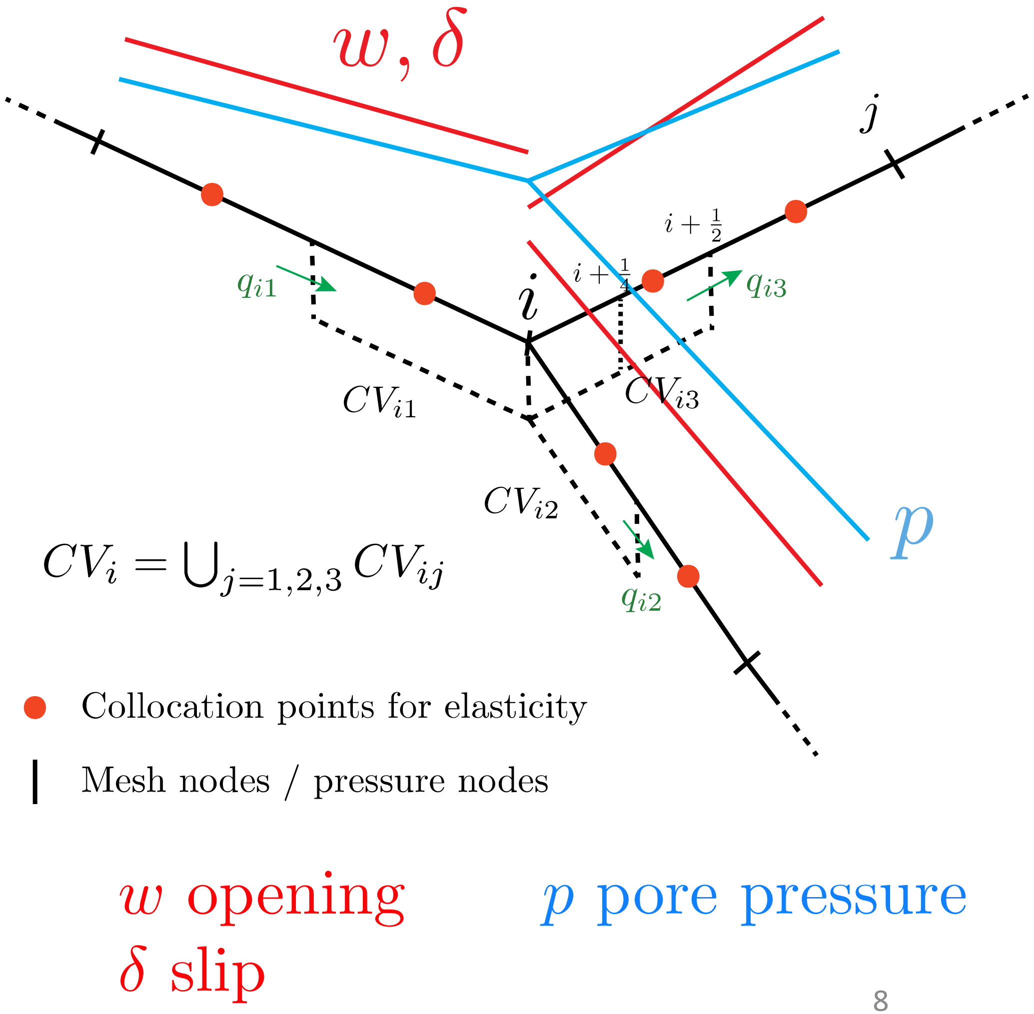

Solution of the equilibrium under constraints

An implicit time-stepping scheme

Yielding loop

$$\mathcal{S}_{inact.} \notin \{\mathcal{S}_{a,I} \cup \mathcal{S}_{a,II} \cup \mathcal{S}_{interp.}\}$$

Solution of balance of momentum & constraints

$$\begin{cases} \mathbf{t}^{\prime,n+1} = \mathbf{t}^{o} + \mathbf{E}_{\mathcal{H}}\mathbf{d}^{n+1} - \mathbf{p}_{coll}^{n+1} & 4n_{elts} \text{ Equations} \\ \text{Constraints on DD segments} & 4n_{elts} \text{ Equations} \end{cases}$$

Fixed point iterative scheme combined with under-relaxation

Solution of the tangent system

Displacement discontinuity method for elasticity

$$\underbrace{\begin{bmatrix} \mathbf{E}_{\mathcal{H}} & \mathbf{I} \\ \mathbf{B} & \mathbf{C} \end{bmatrix}}_{\mathbf{A}} \underbrace{\begin{bmatrix} \Delta \mathbf{d} \\ \mathbf{t}'^{,n+1} \end{bmatrix}}_{\mathbf{x}} = \underbrace{\begin{bmatrix} \mathbf{t}^{o} + \mathbf{E}_{\mathcal{H}} \mathbf{d}^{n} - \mathbf{p}_{coll}^{n+1} \\ \mathbf{a} \end{bmatrix}}_{\mathbf{y}}$$

It's ill-conditioned ☹

GMRES iterative solver

Finite volume method with fully implicit time integration scheme for fluid flow

$$\left[\mathbf{V}_{\mathbf{p}} + \mathbf{L}\right] \left[\Delta \mathbf{p}\right] = \left[-\mathbf{L}\left(\mathbf{p}^{n} - \mathbf{p}^{o}\right)\right]$$

Pardiso direct solver

Preconditioner

Upper-triangular preconditioner matrix applied on right side

$$\mathbf{A}\mathbf{P}_{up}^{-1}\mathbf{u} = \mathbf{y}, \qquad \mathbf{u} = \mathbf{P}_{up}\mathbf{x}$$

with

$$\mathbf{P}_{up} = \begin{bmatrix} \mathbf{D}_{\mathbf{E}_\mathcal{H}} & \mathbf{I} \\ \mathbf{0} & \mathbf{S} \end{bmatrix} \qquad \mathbf{P}_{up}^{-1} = \begin{bmatrix} \mathbf{D}_{\mathbf{E}_\mathcal{H}}^{-1} & -\mathbf{D}_{\mathbf{E}_\mathcal{H}}^{-1}\mathbf{S}^{-1} \\ \mathbf{0} & \mathbf{S}^{-1} \end{bmatrix}$$

$$\mathbf{S} = \mathbf{C} - \mathbf{B}\mathbf{D}_{\mathbf{E}_\mathcal{H}}^{-1} \qquad \mathbf{D}_{\mathbf{E}_\mathcal{H}} = \mathrm{Diag}(\mathbf{E}_\mathcal{H})$$

The system of equations can thus be rewritten as

$$\underbrace{\begin{bmatrix} \mathbf{E}_\mathcal{H}\mathbf{D}_{\mathbf{E}_\mathcal{H}}^{-1} & -\mathbf{E}_\mathcal{H}\mathbf{D}_{\mathbf{E}_\mathcal{H}}^{-1}\mathbf{S}^{-1} + \mathbf{S}^{-1} \\ \mathbf{B}\mathbf{D}_{\mathbf{E}_\mathcal{H}}^{-1} & -\mathbf{B}\mathbf{D}_{\mathbf{E}_\mathcal{H}}^{-1}\mathbf{S}^{-1} + \mathbf{C}\mathbf{S}^{-1} \end{bmatrix} \begin{bmatrix} \mathbf{u_1} \\ \mathbf{u_2} \end{bmatrix} = \begin{bmatrix} \mathbf{y_1} \\ \mathbf{y_2} \end{bmatrix},}_{\mathbf{1}} \qquad \underbrace{\begin{bmatrix} \mathbf{D}_{\mathbf{E}_\mathcal{H}} & \mathbf{I} \\ \mathbf{0} & \mathbf{S} \end{bmatrix} \begin{bmatrix} \mathbf{x_1} \\ \mathbf{x_2} \end{bmatrix} = \begin{bmatrix} \mathbf{u_1} \\ \mathbf{u_2} \end{bmatrix}}_{\mathbf{2}}$$

Preconditioner (cont'd)

We never want to compute the inverse of the Schur complement **S**, so we make a change of variable

$$\mathbf{z_2} = \mathbf{S}^{-1}\mathbf{u_2}$$

such that the system of equations 1 reduces to

$$\underbrace{\begin{bmatrix} \mathbf{E}_{\mathcal{H}}\mathbf{D}_{\mathbf{E}_{\mathcal{H}}}^{-1} & -\mathbf{E}_{\mathcal{H}}\mathbf{D}_{\mathbf{E}_{\mathcal{H}}}^{-1} + \mathbf{I} \\ \mathbf{B}\mathbf{D}_{\mathbf{E}_{\mathcal{H}}}^{-1} & -\mathbf{B}\mathbf{D}_{\mathbf{E}_{\mathcal{H}}}^{-1} + \mathbf{C} \end{bmatrix}}_{\mathbf{A}_p} \begin{bmatrix} \mathbf{u_1} \\ \mathbf{z_2} \end{bmatrix} = \begin{bmatrix} \mathbf{y_1} \\ \mathbf{y_2} \end{bmatrix}$$

Preconditioner (cont'd)

$$\mathbf{A}$$

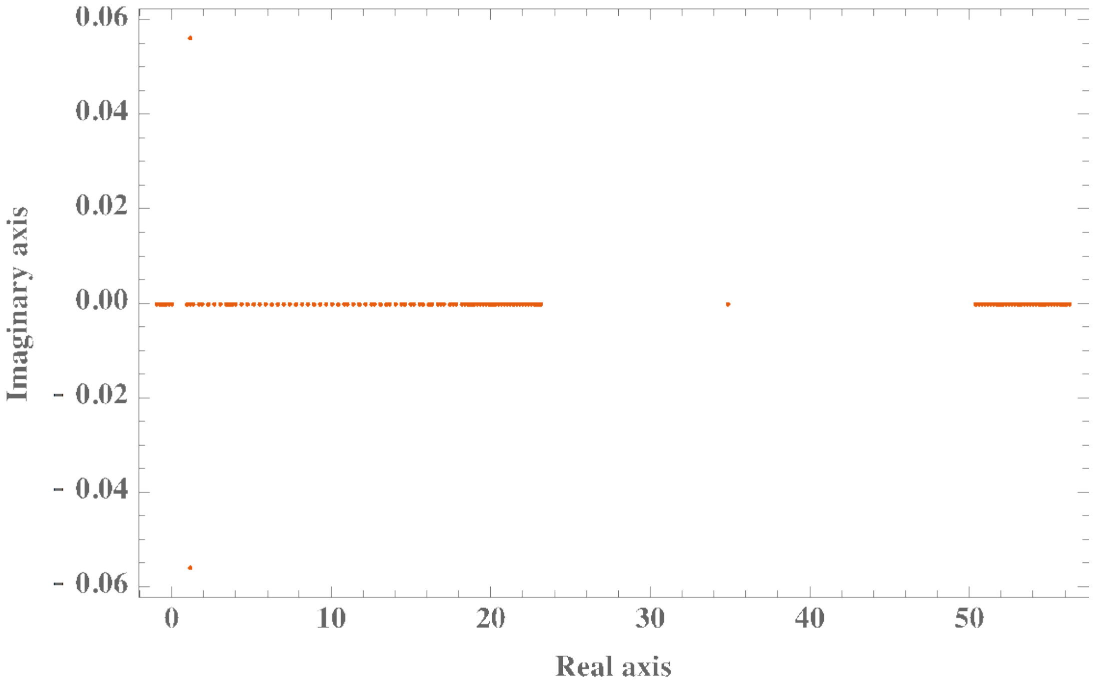

$\rho\left(\mathbf{A}\right) \sim 56.3$ ☹

$$\mathbf{A}_p$$

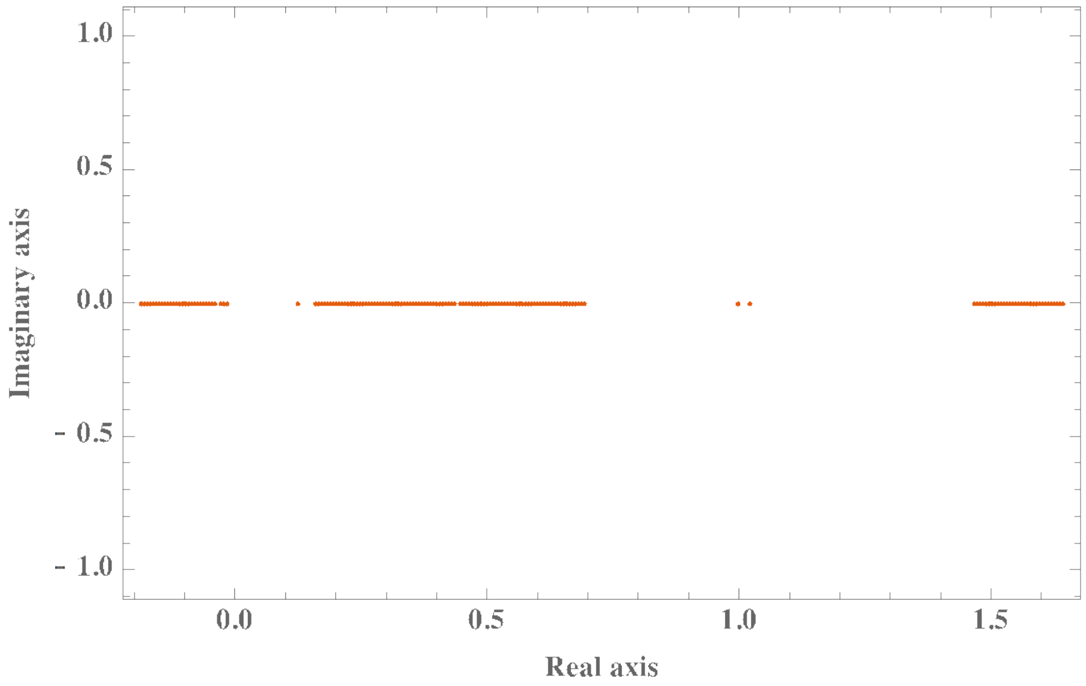

$\rho\left(\mathbf{A}_p\right) \sim 1.64$ ☺

Preconditioner (cont'd)

The preconditioned system of equations is solved via GMRES iterative method for the unknown vectors $\mathbf{u}_1$ and $\mathbf{z}_2$.

Once the iterative solution converges within a given tolerance, the solution of the preconditioned mechanical problem is given by

$$\mathbf{t}'^{,\mathbf{n+1}} = \mathbf{x_2} = \mathbf{z_2}, \qquad \Delta\mathbf{d} = \mathbf{x_1} = \mathbf{D}_{\mathbf{E}_{\mathcal{H}}}^{-1}(\mathbf{u_1} - \mathbf{z_2})$$

No need to solve iteratively 2 system of equations

& no need to invert Schur complement!

Example: tensile wellbore failure

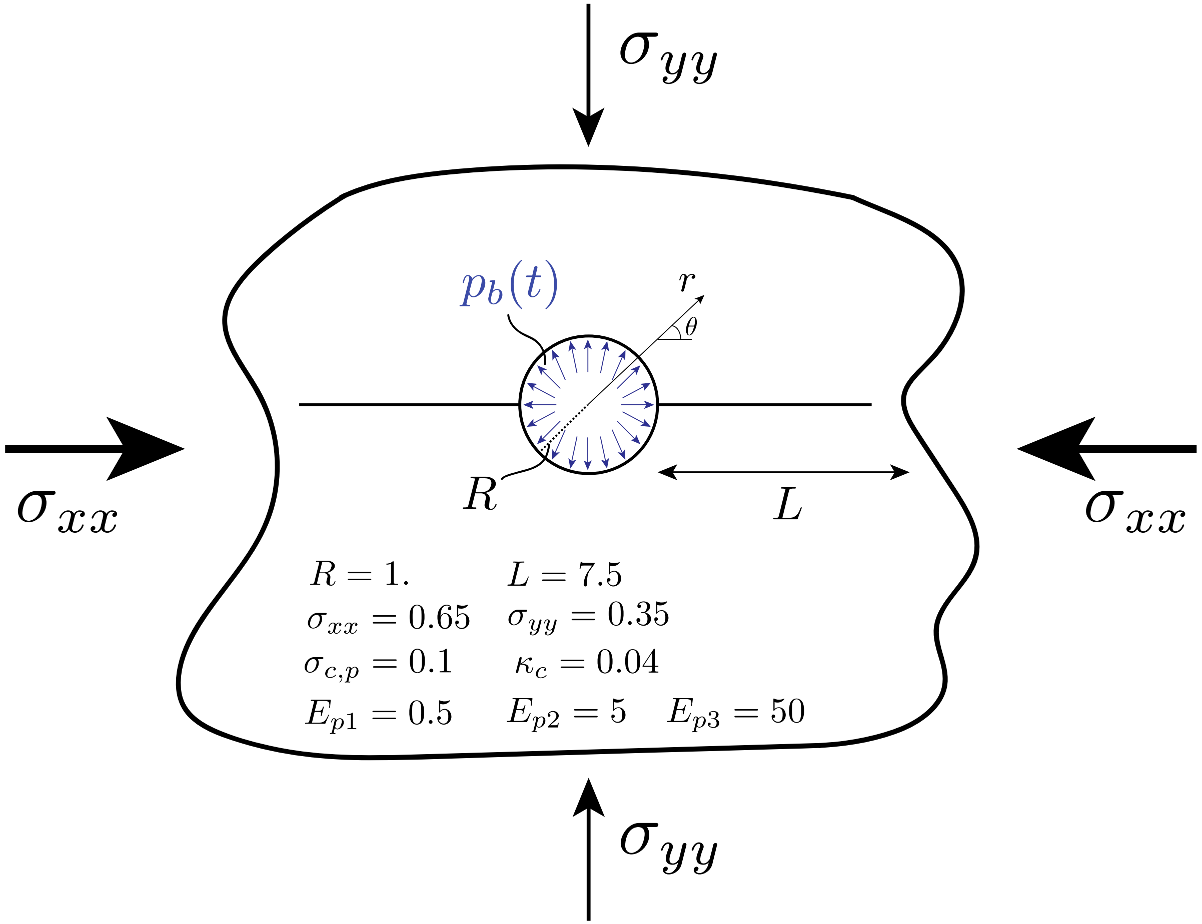

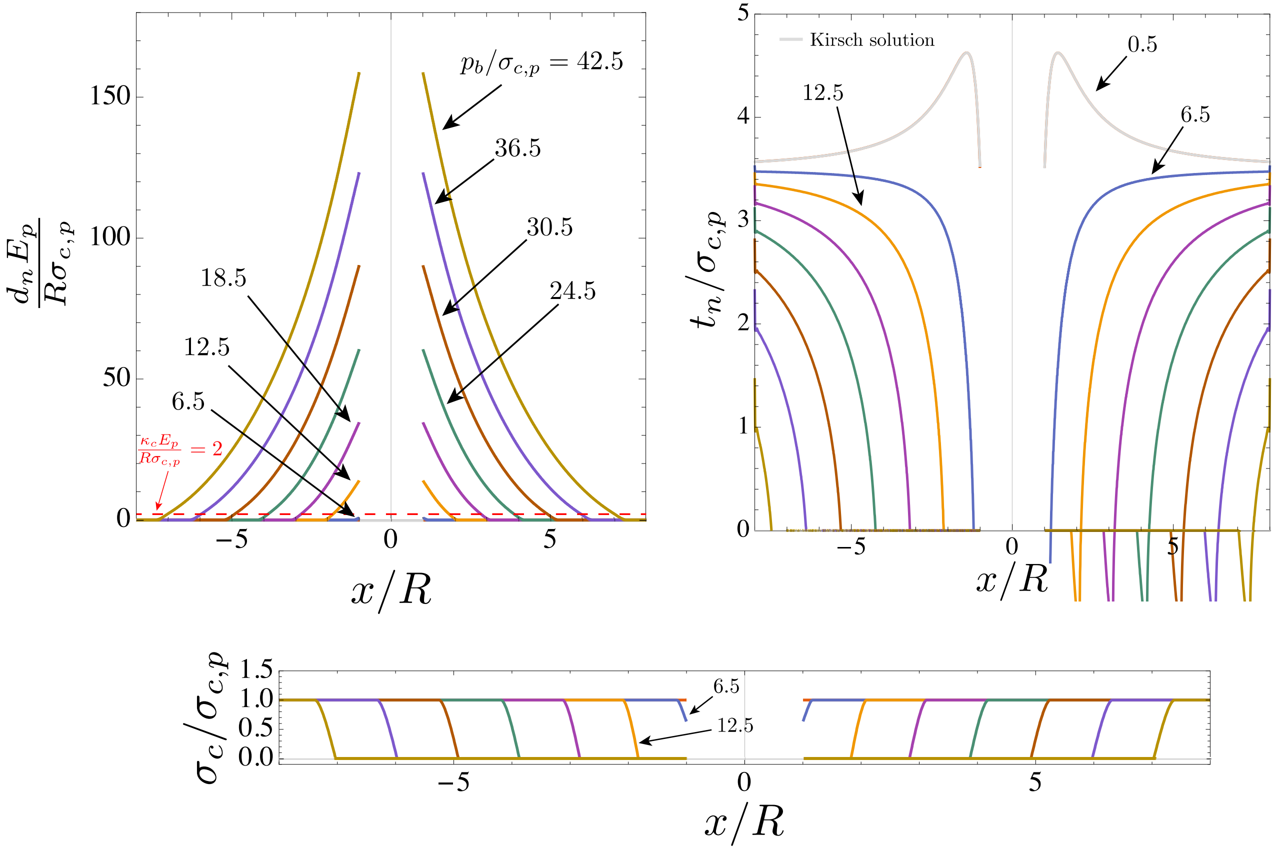

Example: shear-banding in uniaxial compression

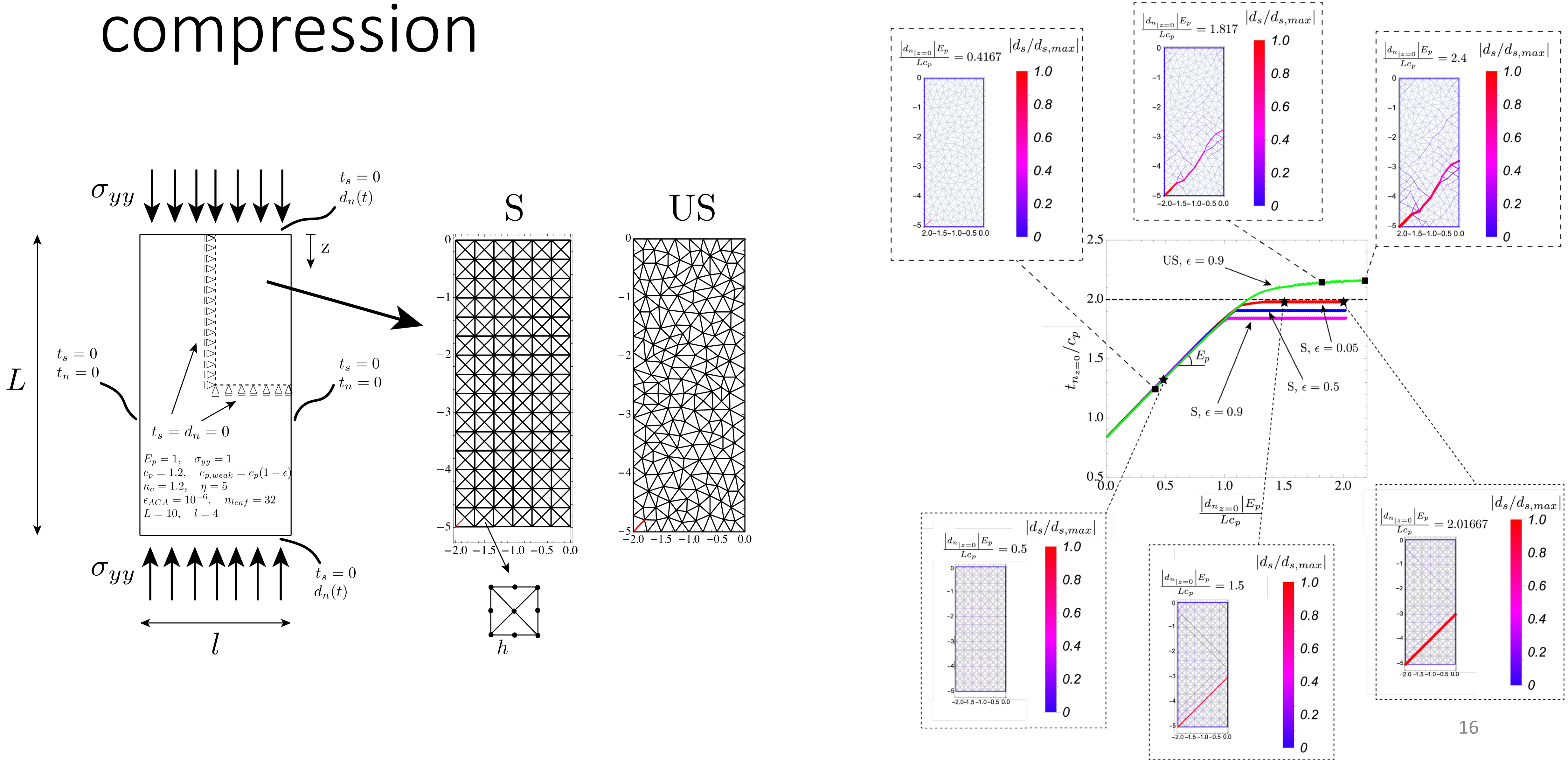

Example: Injection into a Discrete Fracture Network

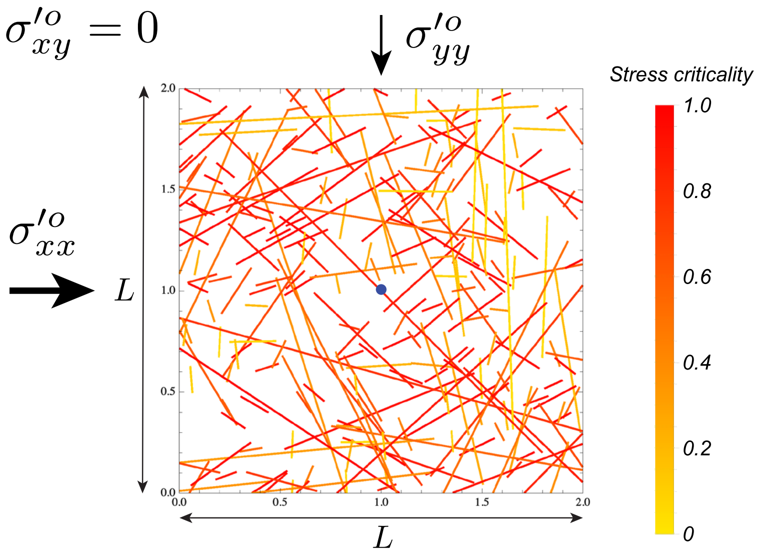

- 251 pre-existing fractures
- Constant friction coefficient

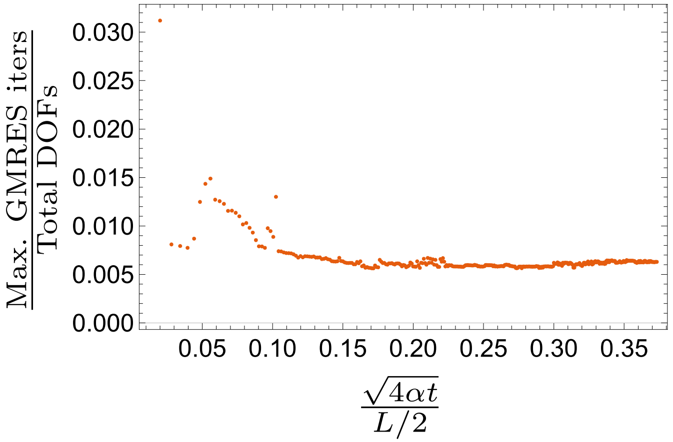

$$\frac{\sqrt{4\alpha t}}{L/2} = 0.139$$

$$\frac{\sqrt{4\alpha t}}{L/2} = 0.241$$

$$\frac{\sqrt{4\alpha t}}{L/2} = 0.373$$

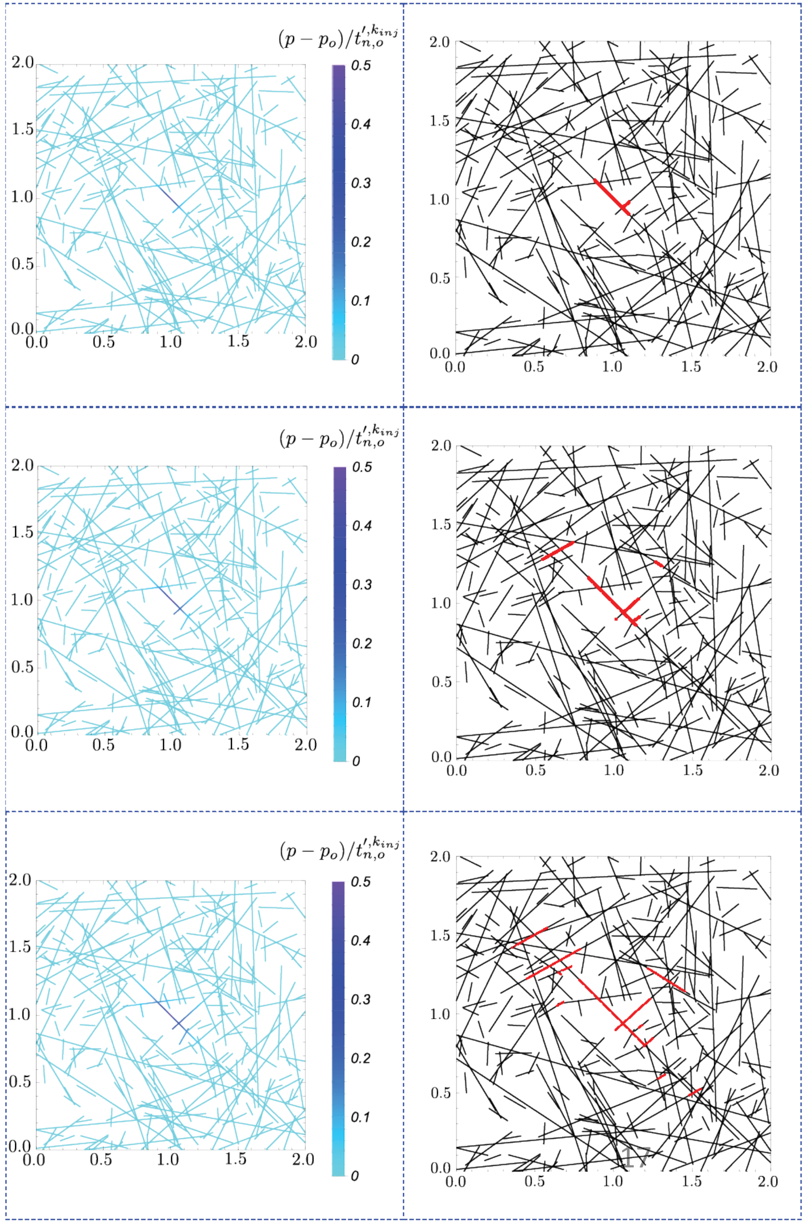

IMPACT OF INJECTION RATE RAMP-UP ON NUCLEATION AND ARREST OF DYNAMIC FAULT SLIP

Motivations

Many numerical and theoretical models have been developed in order to investigate the impact of operational design parameters, such as injection pressure or injection rate, on fault slip development upon fluid injection.

Most of them are Rate and State based models and therefore are well suited to explain features of earthquake cycles and seismicity rates.

Water Resources Research

RESEARCH ARTICLE
10.1029/2018WR023587

Response of Induced Seismicity to Injection Rate Reduction: Models of Delay, Decay, Quiescence, Recovery, and Oklahoma

Key Points:
- We developed models of induced seismicity decay and recovery after an injection rate reduction
- Seismicity, dependent on pressurization rate above a threshold

David Dempsey[1] and Jeremy Riffault[1]
[1]Department of Engineering Science, University of Auckland, Auckland, New Zealand

SCIENCE ADVANCES | RESEARCH ARTICLE

SEISMOLOGY

How will induced seismicity in Oklahoma respond to decreased saltwater injection rates?

Cornelius Langenbruch* and Mark D. Zoback

RESEARCH ARTICLE | JUNE 26, 2018

Seismicity Rate Surge on Faults after Shut-in: Poroelastic Response to Fluid Injection

K. W. Chang; H. Yoon; M. J. Martinez

Bulletin of the Seismological Society of America (2018) 108 (4): 1889–1904.
https://doi.org/10.1785/0120180054 Article history

RESEARCH ARTICLE | MAY 03, 2017

The Effects of Varying Injection Rates in Osage County, Oklahoma, on the 2016 M_w 5.8 Pawnee Earthquake

Andrew J. Barbour; Jack H. Norbeck; Justin L. Rubinstein

Seismological Research Letters (2017) 88 (4): 1040–1053.
https://doi.org/10.1785/0220170003 Article history

JGR Solid Earth

RESEARCH ARTICLE
10.1029/2019JB017898

Effect of the Injection Scenario on the Rate and Magnitude Content of Injection-Induced Seismicity: Case of a Heterogeneous Fault

Key Points:
- We investigate the effect of the fluid injection scenario on the features of induced seismic activity
- The seismicity rate and the pore pressure rate are temporally

Almakari Michelle[1], Dublanchet Pierre[1], Chauris Hervé[1], and Pellet Frédéric[1]
[1]MINES ParisTech, PSL University, Centre de géosciences, Fontainebleau, France

Geophysical Research Letters

RESEARCH LETTER
10.1029/2020GL089426

Effect of Pressure Rate on Rate and State Frictional Slip

Key Points:
- Rapid slip events occur during the duration of a representative experiment in a limited range of pressure rate and diffusivity

J. W. Rudnicki[1] and Y. Zhan[2]
[1]Department of Civil and Environmental Engineering and Department of Mechanical Engineering, Northwestern University, Evanston, IL, USA, [2]School of Civil and Resource Engineering, University of Science and Technology Beijing, Beijing, China

Motivations

Even laboratory experiments..

Geophysical Research Letters

RESEARCH LETTER
10.1029/2019GL086627

Laboratory Study on Fluid-Induced Fault Slip Behavior: The Role of Fluid Pressurization Rate

Lei Wang[1,2], Grzegorz Kwiatek[1,2], Erik Rybacki[1], Audrey Bonnelye[1], Marco Bohnhoff[1,2], and Georg Dresen[1,3]

[1]Helmholtz Centre Potsdam, GFZ German Research Centre for Geosciences, Potsdam, Germany, [2]Department of Earth Sciences, Free University Berlin, Berlin, Germany, [3]Institute of Earth and Environmental Science, University of Potsdam, Potsdam, Germany

Key Points:
- Fluid-induced fault slip experiments have been conducted on critically stressed sandstone samples with saw-cut fractures
- Fluid-induced fault slip mode is controlled by fluid pressurization rate rather than by the magnitude of

Geophysical Research Letters

RESEARCH LETTER
10.1002/2016GL068893

Fault slip controlled by stress path and fluid pressurization rate

Melodie E. French[1], Wenlu Zhu[1], and Jeremy Banker[1]

[1]Department of Geology, University of Maryland, College Park, Maryland, USA

Key Points:
- Fluid pressurization is less effective at inducing accelerated slip events than

JGR Solid Earth

RESEARCH ARTICLE
10.1029/2019JB018517

Fault Reactivation During Fluid Pressure Oscillations: Transition From Stable to Unstable Slip

Corentin Noël[1], François X. Passelègue[1], Carolina Giorgetti[1], and Marie Violay[1]

[1]Laboratory of Experimental Rock Mechanics, Ecole Polytechnique Fédérale de Lausanne, Lausanne, Switzerland

Key Points:
- Laboratory investigation of the effect of fluid pressure oscillations on the fault stability behavior

Motivations

The impact of fluid pressurization on nucleation and potential arrest of dynamic slip on a frictional weakening fault has been extensively investigated by Garagash & Germanovich (2012) using a 2D fault model and by Galis et al. (2017) with a similar model but in 3D.

However, their generic findings are valid for two types of fault pressurizations:

- constant over-pressure
- constant injection rate

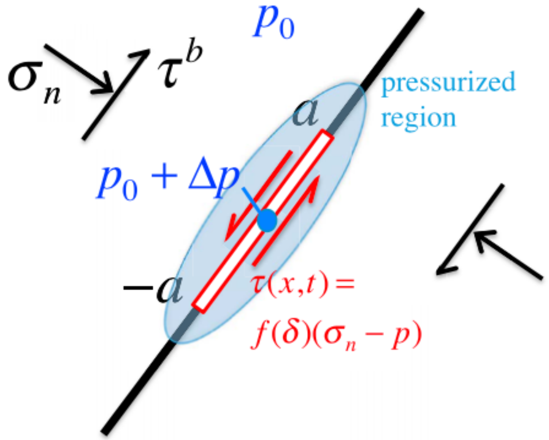

[Taken from Garagash and Germanovich, *JGR*, 2012]

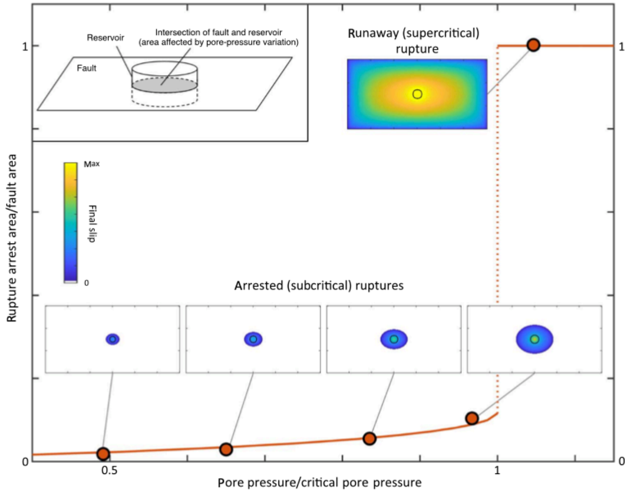

[Taken from Galis at al., *Science Advances*, 2017]

Motivations

Many injection protocols used in hydro-shearing fault experiments include stimulation cycles where either injection pressure or injection rate increases in a stepwise manner up to reach a steady state value, followed then by a shut-in phase.

EXPERIMENT AT GRIMSEL TEST SITE (2017)

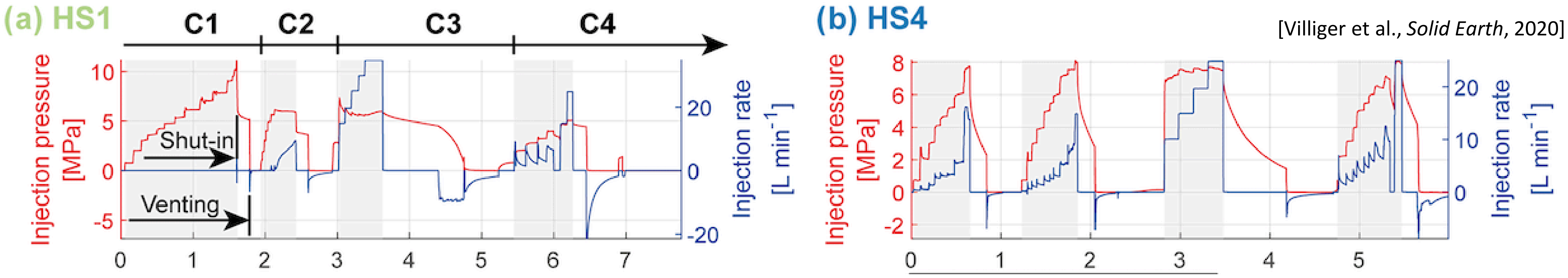

[Villiger et al., *Solid Earth*, 2020]

2019 STIMULATION AT FORGE SITE (UTAH) WELL 58-32

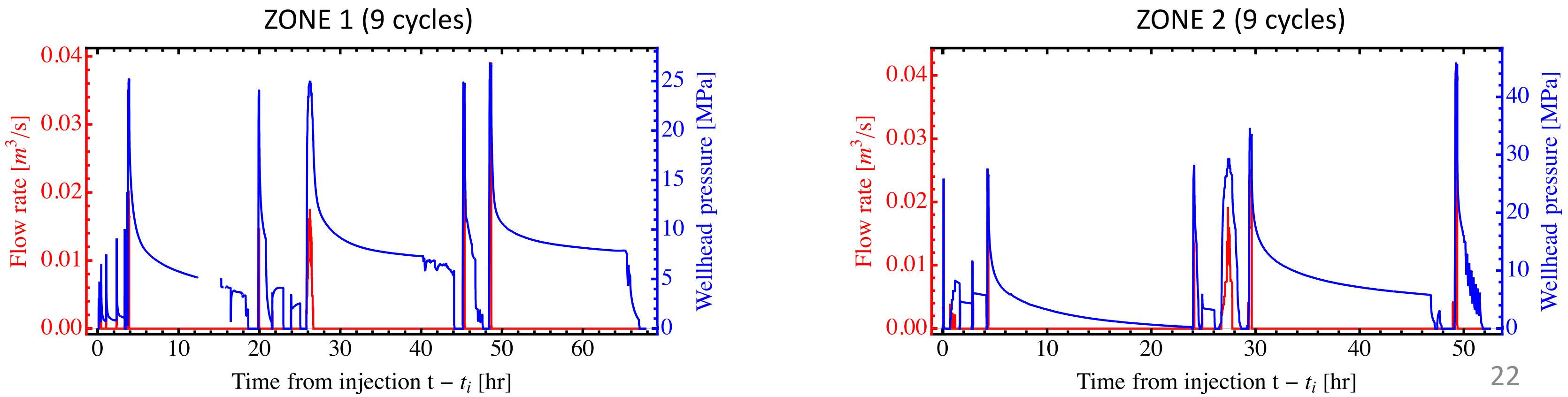

Motivations

- How does the injection rate ramp-up impact the nucleation and potential arrest of dynamic slip on a frictional weakening fault?
- Under which condition the pressurization rate plays a role on fault slip propagation?
- In this contribution we address these questions using a simplified injection strategy

Stimulation of Nov. 2020 at the Bedretto Underground Laboratory
Injection interval 12

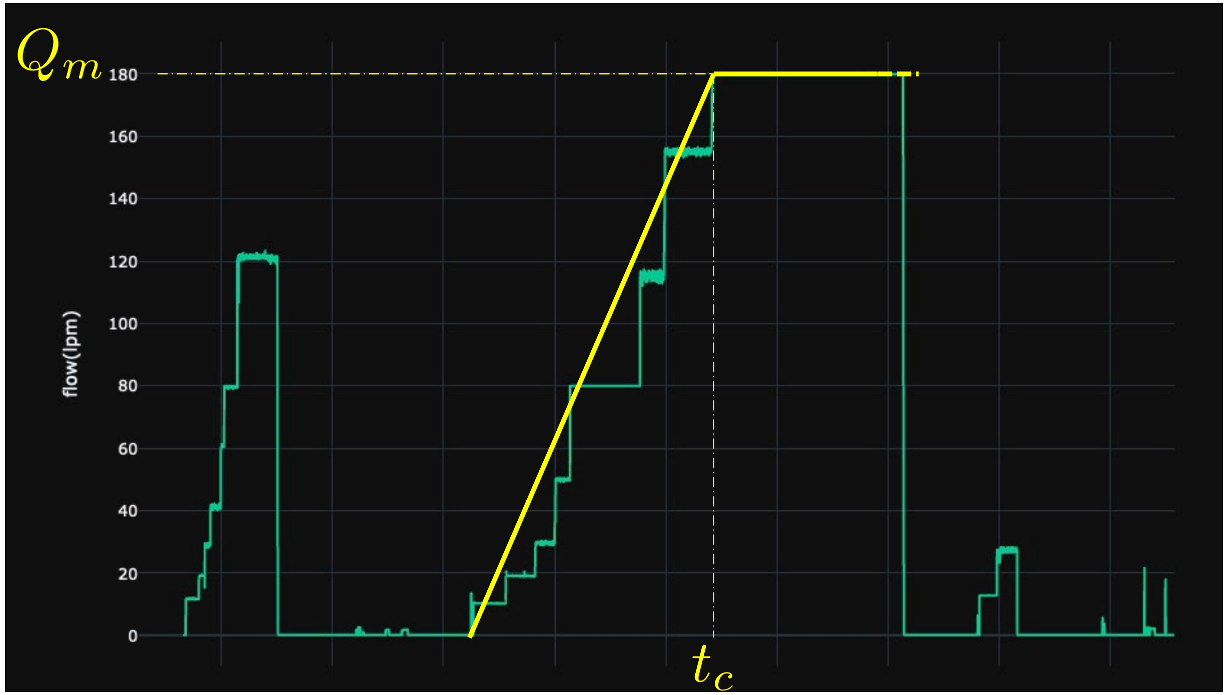

Fault model

HM Coupling

- Quasi-static equilibrium

$$\tau(x,t) = \tau^o - \frac{E_p}{4\pi}\int_{a_-(t)}^{a_+(t)} \frac{\partial\delta(\zeta,t)/\partial\zeta}{\zeta - x}\mathrm{d}\zeta$$

- Constitutive law for frictional slip

$$\tau(x,t) = f(\delta)\left(\sigma_n - \bar{p}(x,t)\right), \quad |x| \le a(t)$$

$$\bar{p}(x,t) = p(x,t) - p_o$$

- Over-pressure diffusion

$$w_h c_f \frac{\partial \bar{p}}{\partial x} + \frac{\partial w_h v}{\partial x} = 0, \qquad v = -\frac{k_f}{\mu}\frac{\partial \bar{p}}{\partial x}$$

$$w_h v = \pm\frac{Q(t)}{2}, \qquad \text{at} \quad x = 0^{\pm}$$

$$\frac{\bar{p}(0,t)}{\sigma'_o} < 1, \quad \forall t$$ No Hydraulic fracturing

$$\alpha = \frac{k_f}{\mu c_f}$$ Fault hydraulic diffusity [L^2T^{-1}]

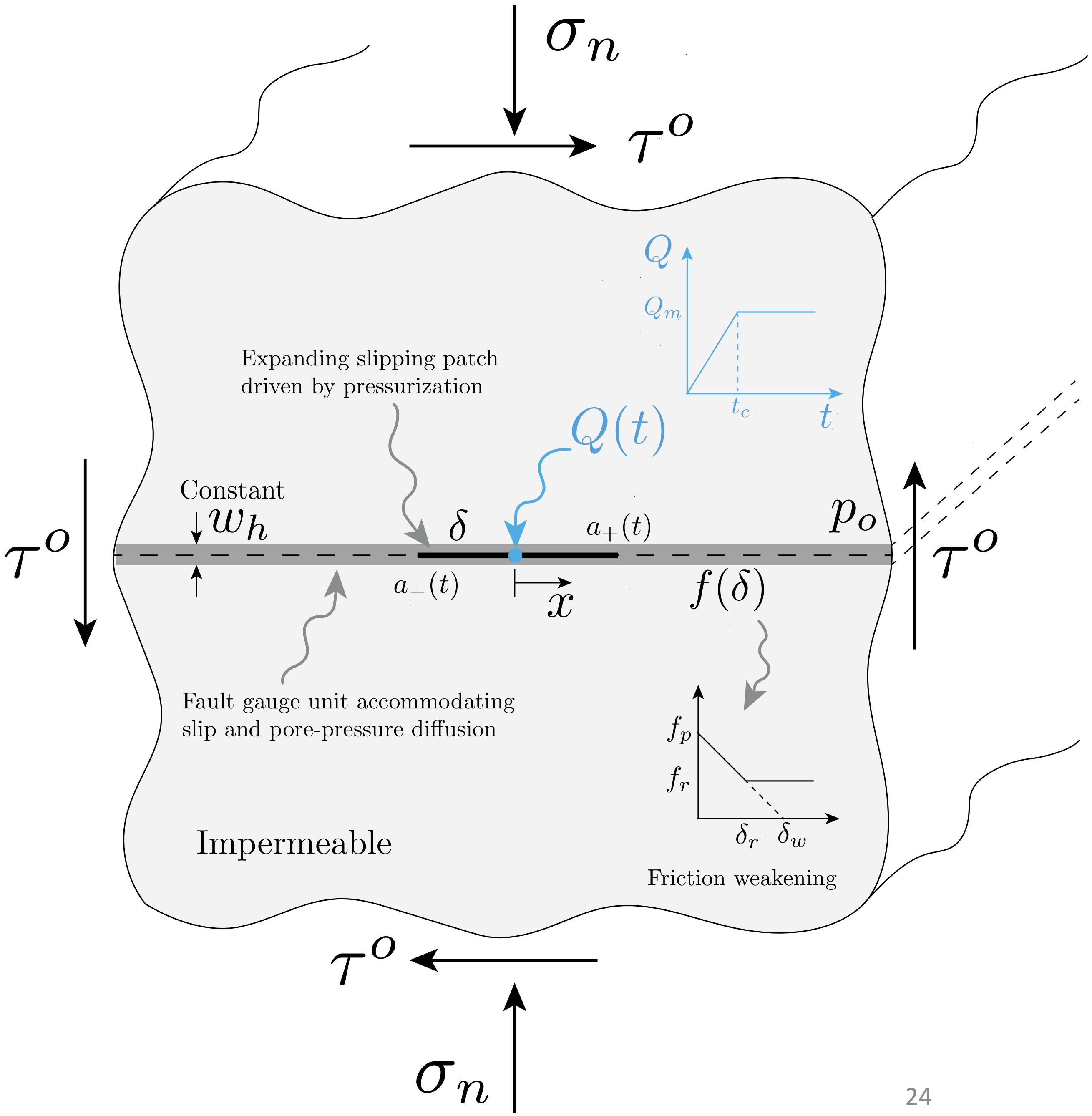

Fault model

HM Coupling

- Quasi-static equilibrium

$$\tau(x,t) = \tau^o - \frac{E_p}{4\pi}\int_{a_-(t)}^{a_+(t)} \frac{\partial\delta(\zeta,t)/\partial\zeta}{\zeta - x}\mathrm{d}\zeta$$

- Constitutive law for frictional slip

$$\tau(x,t) = f(\delta)\left(\sigma_n - \bar{p}(x,t)\right), \quad |x| \leq a(t)$$

$$\bar{p}(x,t) = p(x,t) - p_o$$

- Over-pressure diffusion

$$\begin{cases} \bar{p}(\xi, t \leq t_c) = \underbrace{\left(\frac{2Q_m\mu\sqrt{\alpha}t^{3/2}}{3k_f\sqrt{\pi}t_c w_h}\right)}_{\Delta P(t)} \cdot \underbrace{\left(\mathrm{e}^{-\xi^2}\left(1+\xi^2\right) - \sqrt{\pi}\,|\xi|\left(\frac{3}{2}+\xi^2\right)\mathrm{Erfc}(|\xi|)\right)}_{\Psi(\xi)} \\ \bar{p}(x, t > t_c) = \int_{-\infty}^{\infty} G(x-x', t-t_c)\cdot\bar{p}\left(\frac{x'}{\sqrt{4\alpha t_c}}, t_c\right)\mathrm{d}x' + \frac{\alpha Q_m \mu}{w_k k_f}\int_{t'=t_c}^{t} G(x, t-t')\mathrm{d}t' \end{cases}$$

$$G(x-x', t-t') = \frac{1}{\sqrt{4\pi\alpha(t-t')}}\mathrm{e}^{-\frac{(x-x')^2}{4\alpha(t-t')}} \quad \text{for} \quad t-t' \geq 0 \qquad \xi = \frac{x}{\sqrt{4\alpha t}}$$

[Carslaw & Jaeger, 1959]

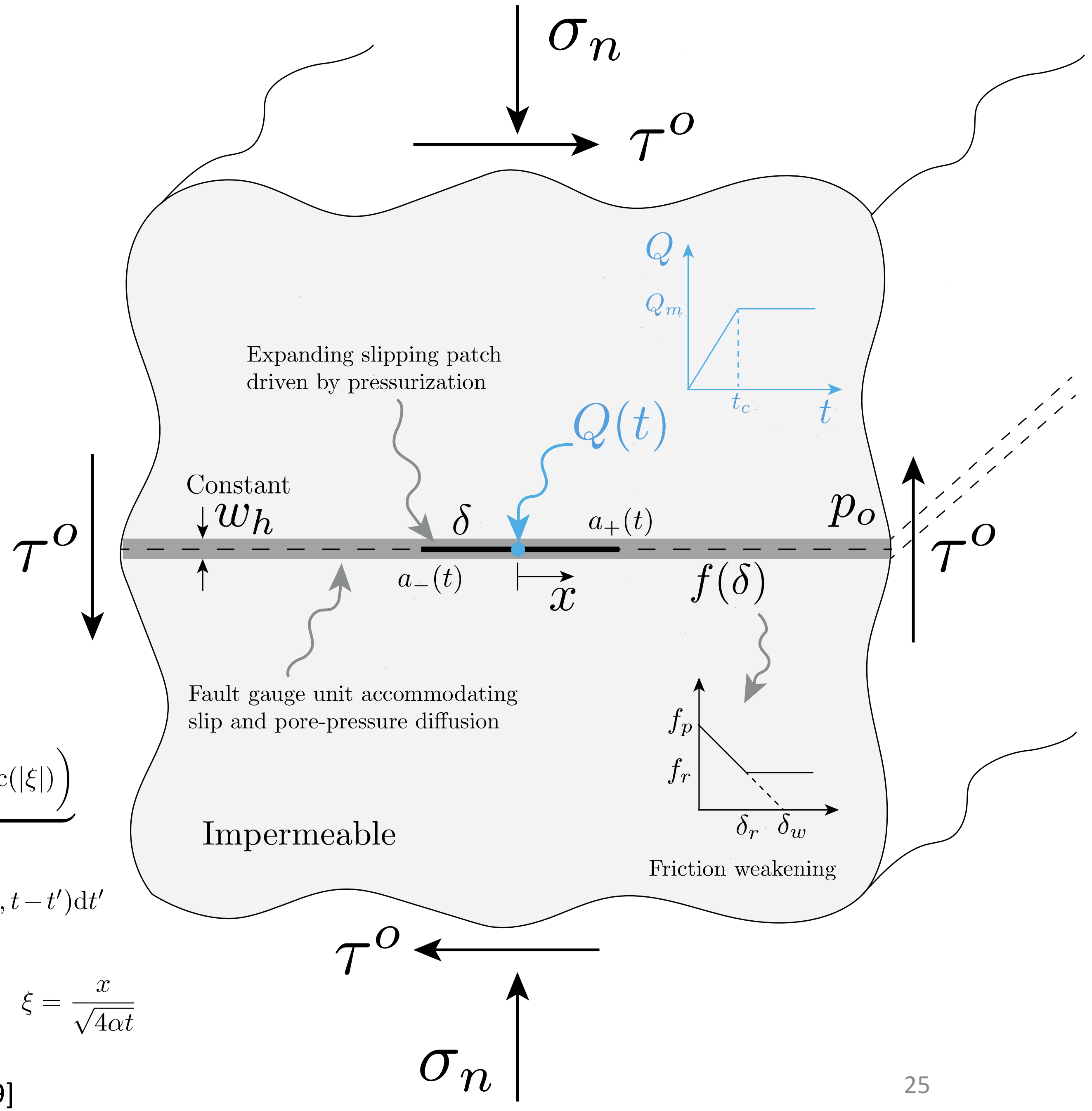

Scaling analysis

It is a powerful technique when applied on physic-based models. It can help systematic investigations of all the physical processes occurring.

Upon introducing the following characteristic scales in the governing equations

$$\tau(x,t) = \tau_p \cdot \mathcal{T}(x,t), \qquad \delta(x,t) = \delta_w \cdot \Delta(x,t), \qquad \bar{p}(x,t) = \sigma_o' \cdot \Pi(x,t), \qquad x = a \cdot \mathcal{X} \qquad t = t_w \cdot \mathrm{T}$$

We obtain

$$\mathcal{T}(a\mathcal{X},t) = \frac{\tau^o}{\tau_p} - \frac{1}{2\pi}\frac{a_w}{a}\int_{-1}^{1} \frac{\partial \Delta(a\mathcal{X},t)}{\partial \zeta}\frac{\mathrm{d}\zeta}{(\zeta/a - \mathcal{X})}$$

$$\mathcal{T}(a\mathcal{X},t) = \frac{f(\delta)}{f_p}\left(1 - \Pi(a\mathcal{X},t)\right)$$

$$\frac{f(\delta)}{f_p} = \begin{cases} 1 - \Delta(a\mathcal{X},t) & \Delta(a\mathcal{X},t) \le 1 - \frac{f_r}{f_p} \\ \frac{f_r}{f_p} & \Delta(a\mathcal{X},t) > 1 - \frac{f_r}{f_p} \end{cases}$$

$$\frac{\partial \Pi}{\partial \mathrm{T}} - \frac{1}{4}\frac{\partial^2 \Pi}{\partial \mathcal{X}^2} = 0$$

$$\left.\frac{\partial \Pi}{\partial \mathcal{X}}\right|_{\mathcal{X}=0^{\pm}} = \begin{cases} \pm\frac{Q_m}{Q^*}\frac{t_w}{t_c}\cdot \mathrm{T} & \mathrm{T} \le \frac{t_c}{t_w} \\ \pm\frac{Q_m}{Q^*} & \mathrm{T} > \frac{t_c}{t_w} \end{cases}$$

$$a_w = \frac{E_p}{2\tau_p}\delta_w \sim \left[10^{-1}\mathrm{m}, 10^{1}\mathrm{m}\right] \quad \text{Slipping patch length-scale}$$

$$t_w = \frac{a_w^2}{4\alpha} \sim \left[10^{0}\mathrm{min}, 10^{2}\mathrm{min}\right] \quad \text{Diffusion time scale}$$

$$Q^* = \frac{2\sigma_o' w_h k_f}{a_w \mu} \sim \left[10^{-1}\mathrm{l/s}, 10^{2}\mathrm{l/s}\right] \quad \text{Characteristic injection rate scale}$$

$$\left(\mathcal{T}, \Delta, \Pi, a/a_w\right) = \mathcal{F}\left(\frac{\tau^o}{\tau_p}, \frac{f_r}{f_p}, \frac{Q_m}{Q^*}, \frac{t_c}{t_w}\right)$$

Scaling analysis

- Stress criticality $\frac{\tau^o}{\tau_p}$

$\frac{\tau^o}{\tau_p} \to 1$ Critically stressed / Unstable fault

$\frac{\tau^o}{\tau_p} \to 0$ Marginally pressurized / Ultimately stable fault

$\tau^o \sim \mathrm{MPa}$

$\tau_p = f_p \sigma'_o \sim \mathrm{MPa}$

- Friction weakening ratio $\frac{f_r}{f_p} = 1 - \frac{\delta_r}{\delta_w}$

$\frac{f_r}{f_p} \to 1$ Low frictional weakening condition

$\frac{f_r}{f_p} \to 0$ Large frictional weakening condition

$\delta_r \sim \left[10^{-4}\mathrm{m}, 10^{-3}\mathrm{m}\right]$

$\delta_w \sim \left[10^{-4}\mathrm{m}, 10^{-2}\mathrm{m}\right]$

- Normalized maximum injection rate $\frac{Q_m}{Q^*}$

$10^{-1} \lesssim \frac{Q_m}{Q^*} \lesssim 10^1 \to$ Typical for hydro-shearing

$\frac{Q_m}{Q^*} \gg 1 \to$ Typical for hydraulic fracturing

$Q_m \sim \left[10^2 \mathrm{l/s}, 10^{-1} \mathrm{l/s}\right]$

$Q^* = \frac{2\sigma'_o w_h k_f}{a_w \mu} \sim \left[10^{-1} \mathrm{l/s}, 10^2 \mathrm{l/s}\right]$

- Normalized ramp-up time scale $\frac{t_c}{t_w}$

$t_c/t_w \ll 1 \to$ Fast ramp-up of injection rate

$t_c/t_w \gg 1 \to$ Slow ramp-up of injection rate

$t_c \sim \left[10^0 \mathrm{min}, 10^3 \mathrm{min}\right]$

$t_w = \frac{a_w^2}{4\alpha} \sim \left[10^0 \mathrm{min}, 10^2 \mathrm{min}\right]$

Small Scale Yielding

- If deviations from linearity occur only over a region that is small compared to geometrical dimension, then the elastic Stress-Intensity Factor controls the local deformation field [Rice, 1968 – Palmer and Rice 1973]
- Small Scale Yielding conditions thus occurs when

$$a \gg a_w$$

- The energy release rate *G* at the propagating crack tip must match the fracture energy G_c, i.e.

$$G = G_c$$

- This is an implicit equation that can be solved for the unknown crack length *a*

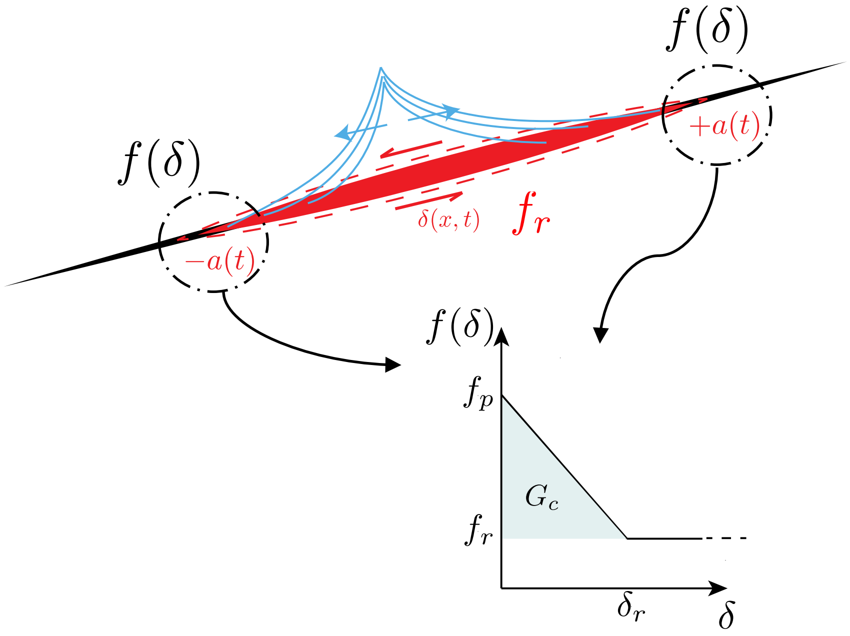

$$G_c = (f_p - f_r)\,\sigma'_o \frac{\delta_r}{2}$$ *Fracture energy*

$$G = \frac{K^2}{E_p}$$ *Energy release rate*

$$K = (\tau^o - \tau_r)\sqrt{\pi a} + \Delta K\,(a,t)$$ *Stress Intensity Factor*

$$\Delta K\,(a,t) = f_r \sqrt{\frac{a}{\pi}} \int_{-a}^{a} \frac{\bar{p}(x,t)}{\sqrt{a^2 - x^2}} \mathrm{d}x$$

$$f_r/f_p = 0.6$$

Ultimately stable fault		Unstable fault
FAST RAMP-UP $t_c/t_w \ll 1$ • Vary $\frac{Q_m}{Q^*}$ • Potential nucleation of dynamic event due to frictional weakening conditions $t_n \gg t_w \gg t_c$	SLOW RAMP-UP $t_c/t_w \gg 1$ • Vary $\frac{Q_m}{Q^*}$ • Potential nucleation of dynamic event due to frictional weakening conditions $t_n \sim t_c \gg t_w$	RELATIVELY SLOW RAMP-UP $t_c/t_w \gtrsim 1$ • Always nucleation of run-away rupture $t_n < t_c$

$$f_r/f_p = 0.6$$

Ultimately stable fault		Unstable fault
FAST RAMP-UP $t_c/t_w \ll 1$ • Vary $\frac{Q_m}{Q^*}$ • Potential nucleation of dynamic event due to frictional weakening conditions $t_n \gg t_w \gg t_c$	SLOW RAMP-UP $t_c/t_w \gg 1$ • Vary $\frac{Q_m}{Q^*}$ • Potential nucleation of dynamic event due to frictional weakening conditions $t_n \sim t_c \gg t_w$	RELATIVELY SLOW RAMP-UP $t_c/t_w \gtrsim 1$ • Always nucleation of run-away rupture $t_n < t_c$

Numerical results: ultimately stable fault – Fast ramp-up

$$\boxed{t_c/t_w \ll 1}$$

- No effect of ramp-up phase
- Slip activation and propagation at constant injection rate
- Benchmark with Garagash & Germanovich, 2012 results

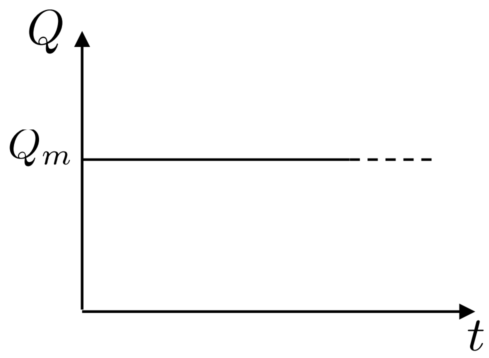

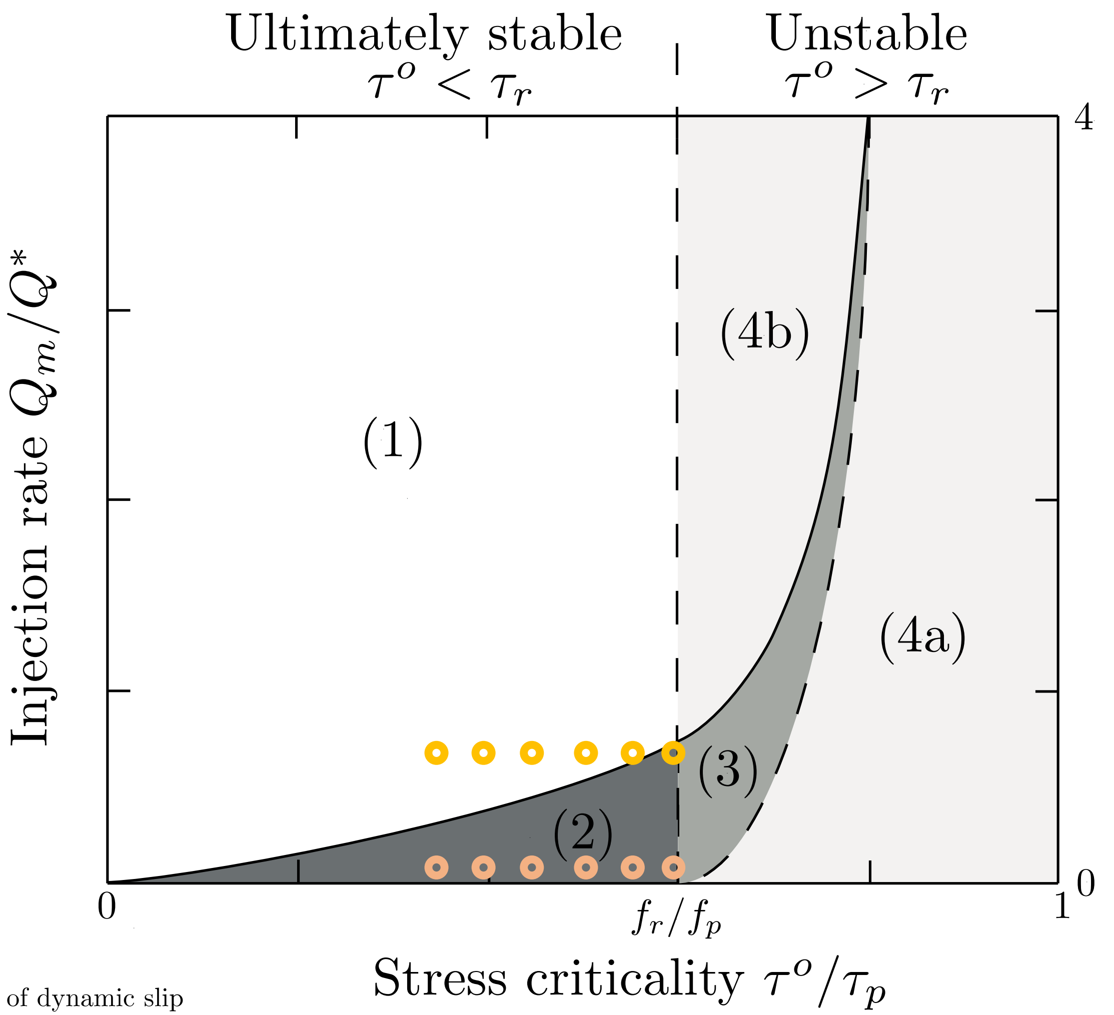

(1) Aseismic slip only
(2) Nucleation and Arrest of dynamic slip
(3) Nucleation, Arrest and re-Nucleation of dynamic slip
(4) Nucleation of dynamic slip

Numerical results: ultimately stable fault – Fast ramp-up

Low maximum injection rate

$Q_m/Q^* = 0.05$

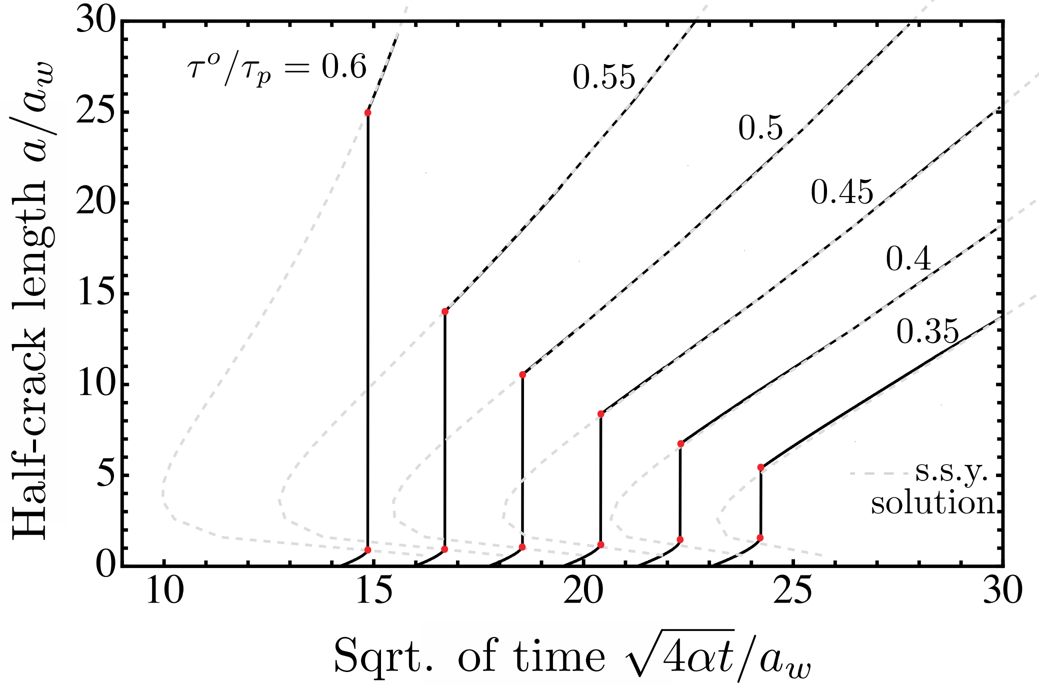

Moderate maximum injection rate

$Q_m/Q^* = 0.5$

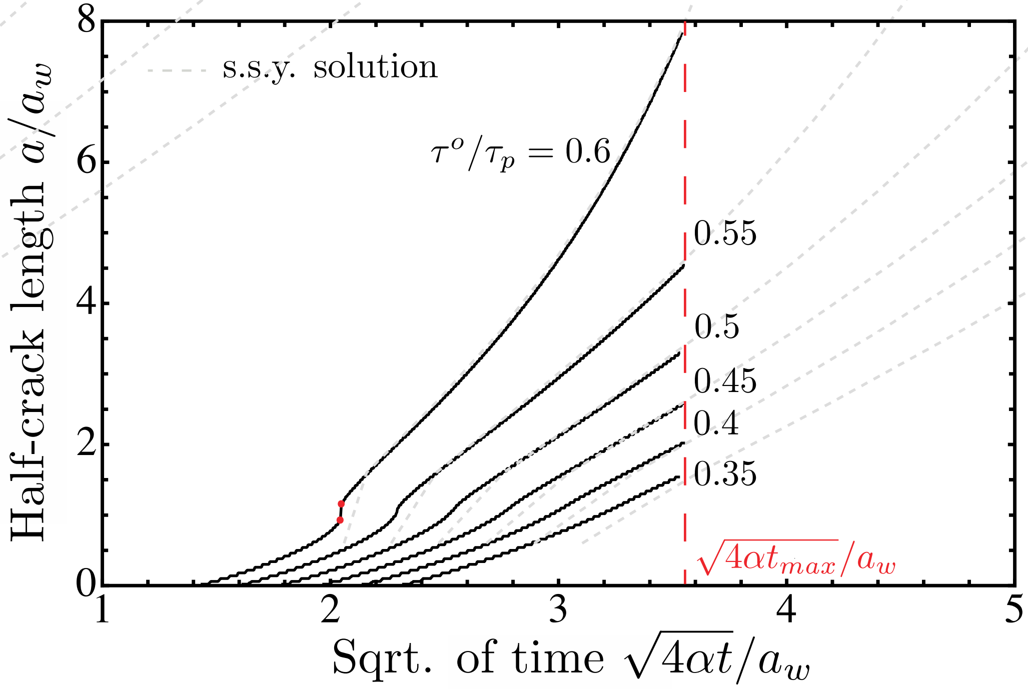

$f_r/f_p = 0.6$ $\quad t_c/t_w = 0.01 \ll 1$

Numerical results: ultimately stable fault – Fast ramp-up

If nucleation follows shortly slip activation, then the shear crack at nucleation time is confined near injection point and is subjected to a uniform over-pressure equal to the minimum value required to activate slip, i.e.

$$\bar{p}\left(x \simeq 0, t_n\right) = \left(\tau_p - \tau^o\right)/f_p$$

Solving for the normalized nucleation time, we get

$$\frac{\sqrt{4\alpha t_n}}{a_w} \simeq \frac{\tau_p - \tau^o}{f_p \Delta P_w} \iff \frac{Q_m}{Q^*} \ll \sqrt{\pi}\left(1 - \frac{\tau^o}{\tau_p}\right)$$

$Q_m/Q^* = 0.05 \quad f_r/f_p = 0.6 \quad t_c/t_w = 0.01 \ll 1$

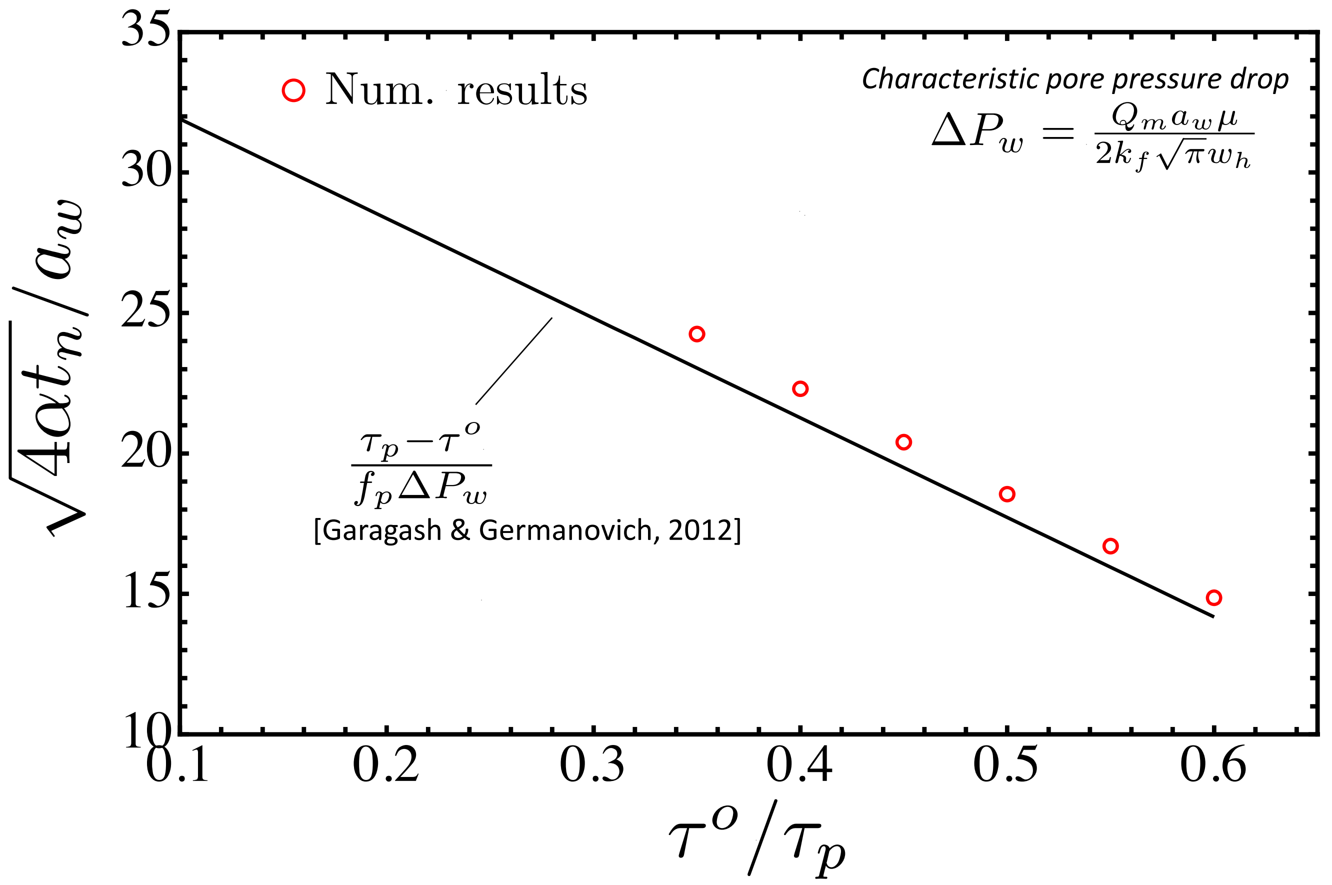

Numerical results: ultimately stable fault – Fast ramp-up

Good match between crack length at nucleation time and corresponding asymptotic solution of Garagash and Germanovich, 2012.

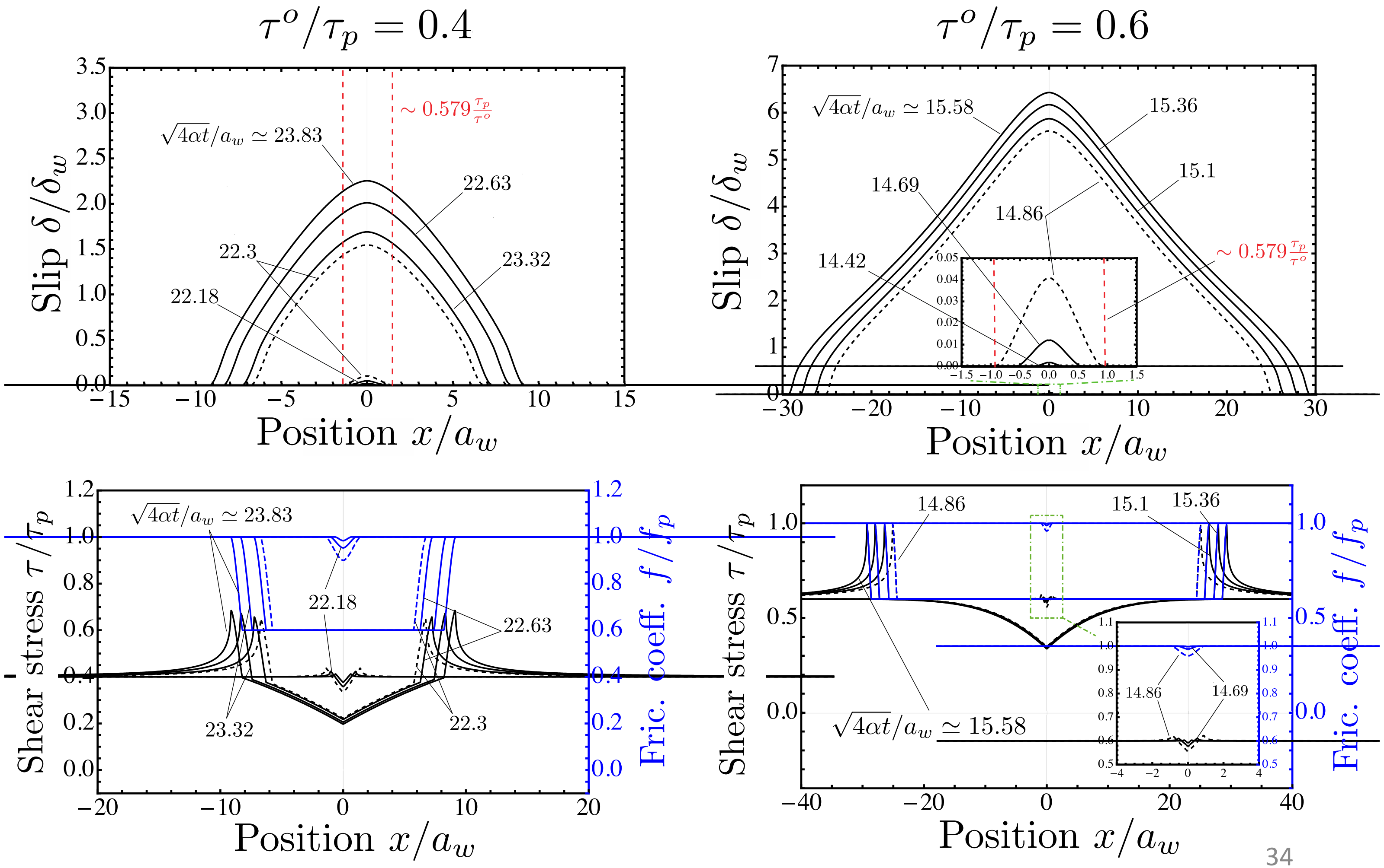

$$f_r/f_p = 0.6$$

Ultimately stable fault		Unstable fault
FAST RAMP-UP $t_c/t_w \ll 1$	SLOW RAMP-UP $t_c/t_w \gg 1$	RELATIVELY SLOW RAMP-UP $t_c/t_w \gtrsim 1$
• Vary $\frac{Q_m}{Q^*}$ • Potential nucleation of dynamic event due to frictional weakening conditions $t_n \gg t_w \gg t_c$	• Vary $\frac{Q_m}{Q^*}$ • Potential nucleation of dynamic event due to frictional weakening conditions $t_n \sim t_c \gg t_w$	• Always nucleation of run-away rupture $t_n < t_c$

Numerical results: ultimately stable fault – Slow ramp-up

Low maximum injection rate

$Q_m/Q^* = 0.05$

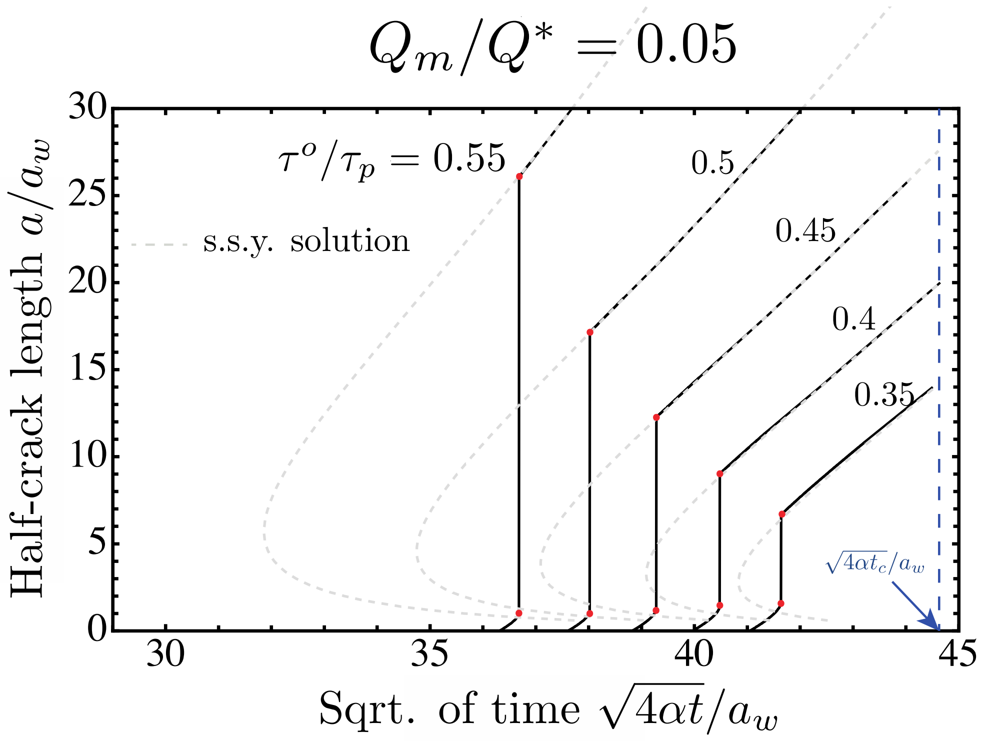

Moderate maximum injection rate

$Q_m/Q^* = 1.$

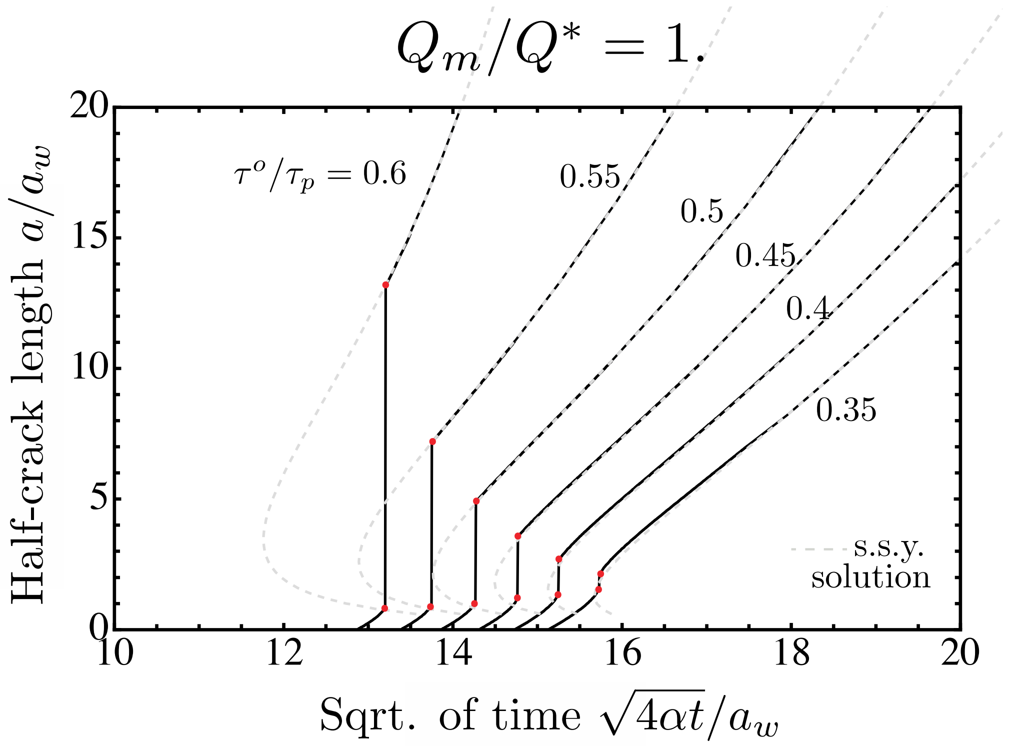

$f_r/f_p = 0.6 \qquad t_c/t_w = 2 \cdot 10^3 \gg 1$

Numerical results: ultimately stable fault – Slow ramp-up

If nucleation follows shortly slip activation, then the shear crack at nucleation time is confined near injection point and is subjected to a uniform over-pressure equal to the minimum value required to activate slip, i.e.

$$\bar{p}\left(x \simeq 0, t_n\right) = \left(\tau_p - \tau^o\right)/f_p$$

Solving for the normalized nucleation time, one get

$$\frac{\sqrt{4\alpha t_n}}{a_w} \simeq \left(\frac{3}{2} \cdot \frac{\tau_p - \tau^o}{f_p \Delta P_w} \cdot \frac{t_c}{t_w}\right)^{1/3} \iff \frac{Q_m}{Q^*} \ll \sqrt{\pi}\left(1 - \frac{\tau^o}{\tau_p}\right)$$

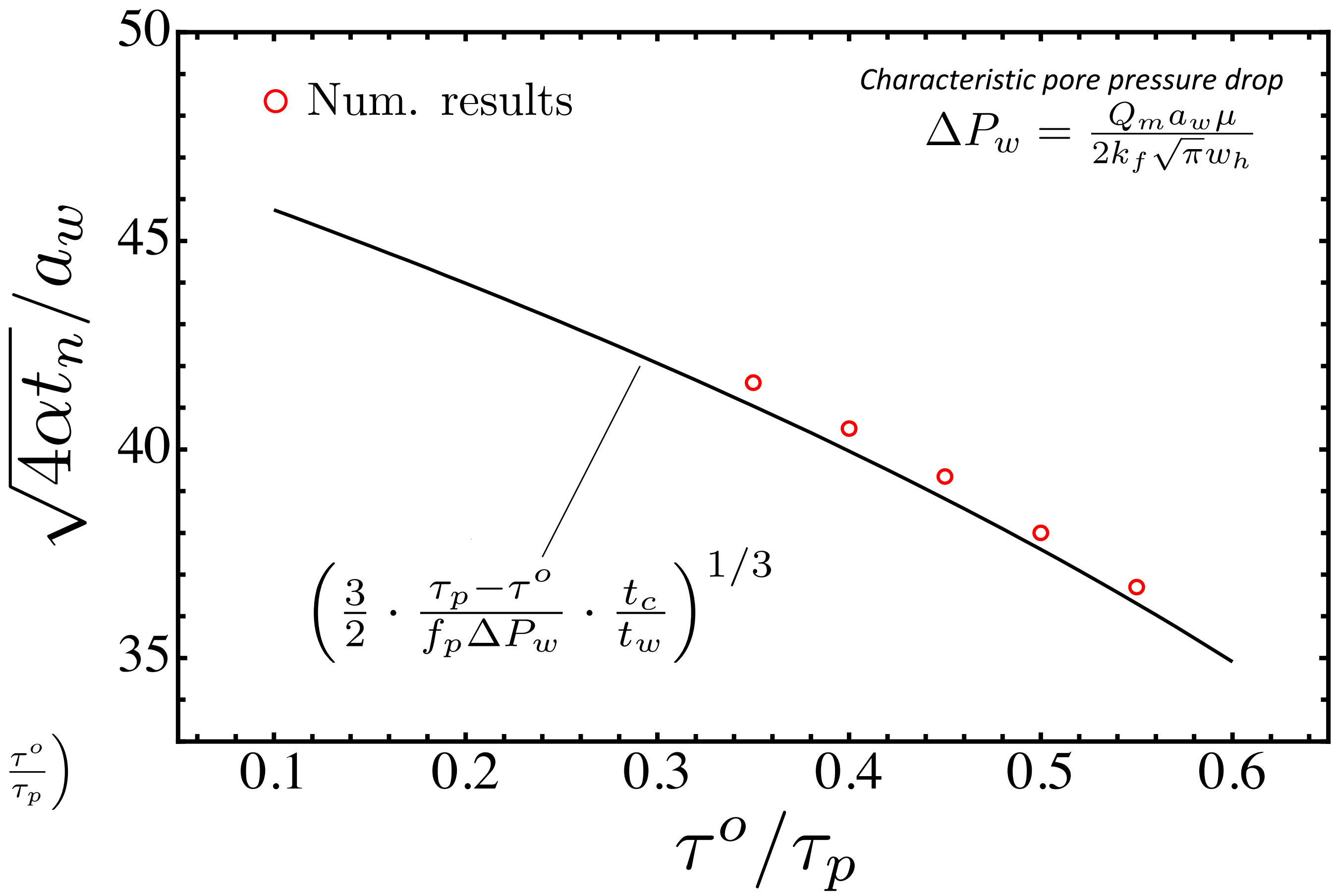

PRESSURIZATION RATE DOES PLAY A ROLE!

Numerical results: ultimately stable fault – Slow ramp-up

- The extent of the arrested dynamic crack is always much larger than the slipping patch length scale a_w and the corresponding nucleation time is known analytically.
- We can calculate analytically the dynamic run-out distance directly from the s.s.y solution resolved at nucleation time.

$\boxed{Q_m/Q^* = 0.05}$

$\boxed{t_c/t_w = 2 \cdot 10^3}$

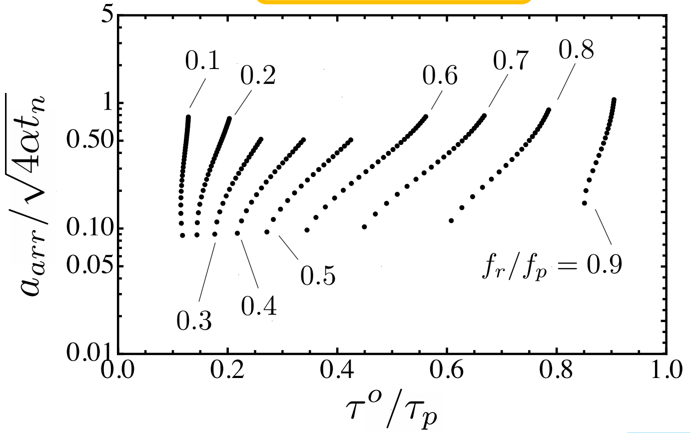

$\boxed{t_c/t_w = 2 \cdot 10^4}$

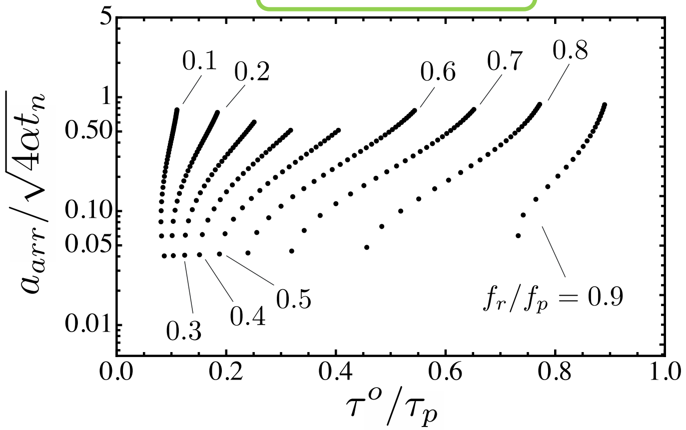

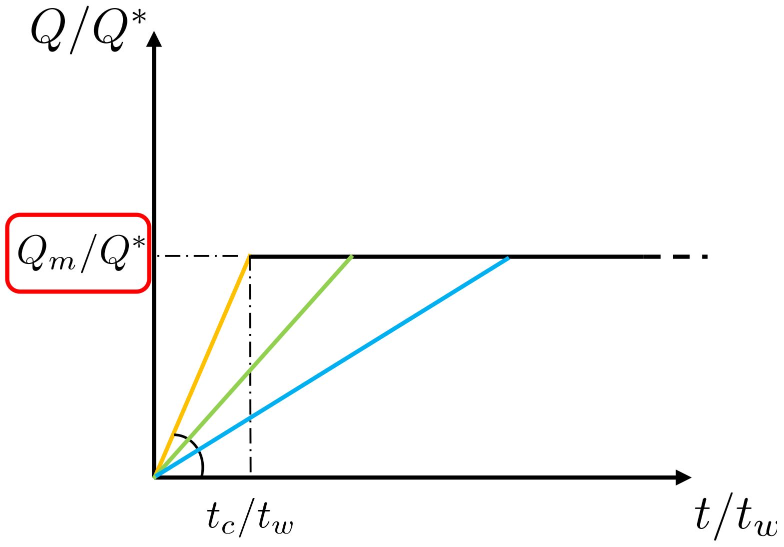

$\boxed{t_c/t_w = 2 \cdot 10^5}$

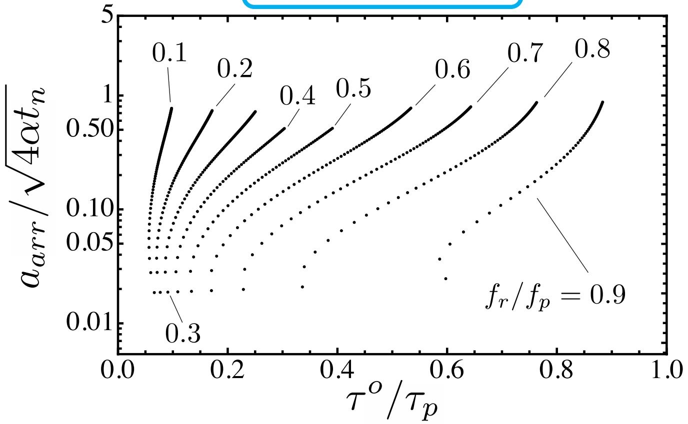

Numerical results: ultimately stable fault – Slow ramp-up

- Power law dependence between dynamic runt-out slip distance and pressurization rate

- LOW PRESSURIZATION RATES LEAD TO LARGER DYNAMIC RUN-OUT DISTANCES!

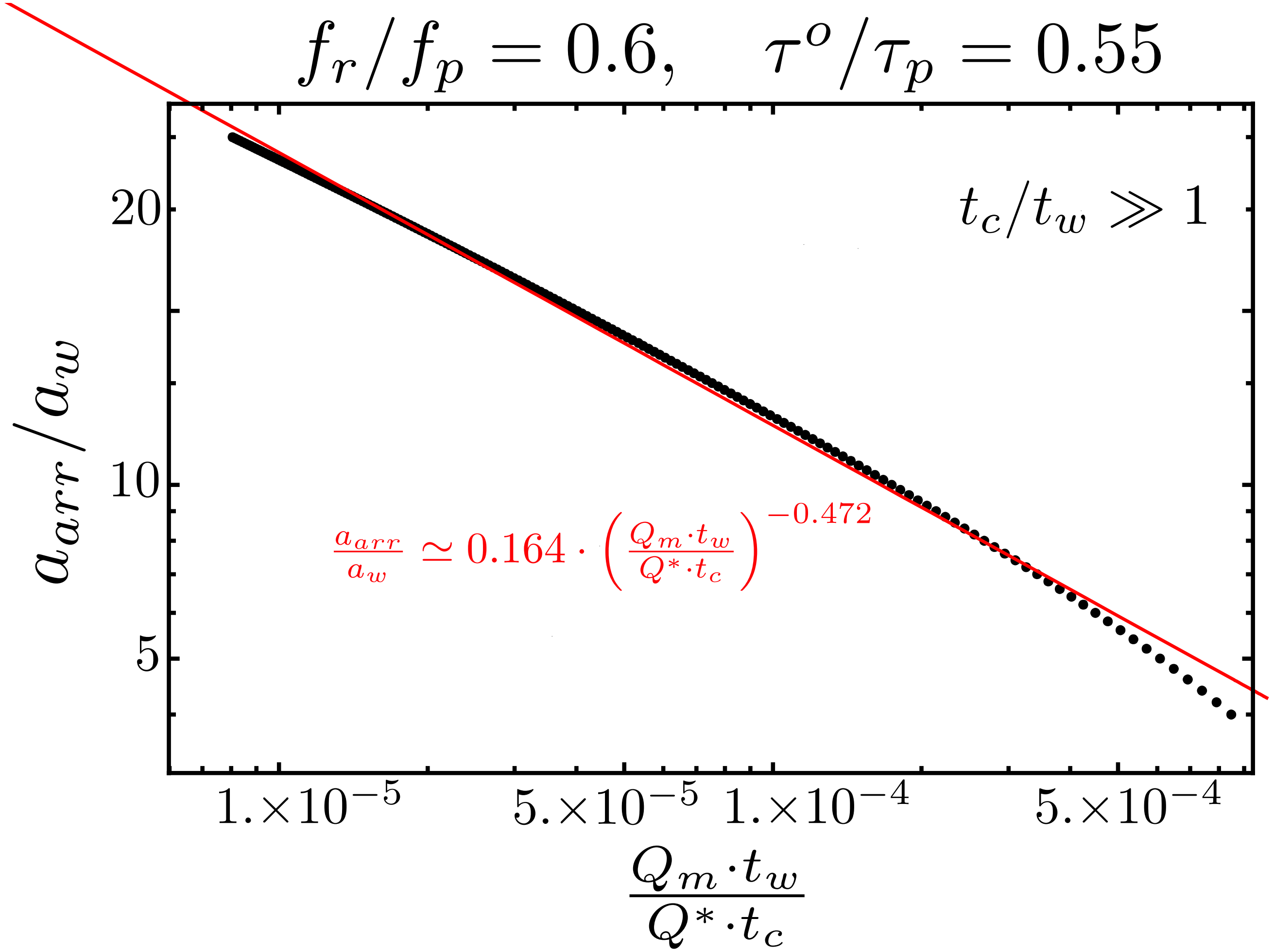

$$f_r/f_p = 0.6$$

Ultimately stable fault		Unstable fault
FAST RAMP-UP $t_c/t_w \ll 1$ • Vary $\frac{Q_m}{Q^*}$ • Potential nucleation of dynamic event due to frictional weakening conditions $t_n \gg t_w \gg t_c$	SLOW RAMP-UP $t_c/t_w \gg 1$ • Vary $\frac{Q_m}{Q^*}$ • Potential nucleation of dynamic event due to frictional weakening conditions $t_n \sim t_c \gg t_w$	RELATIVELY SLOW RAMP-UP $t_c/t_w \gtrsim 1$ • Always nucleation of run-away rupture $t_n < t_c$

Unstable fault

- The fault is critically stressed and thus prompt to fail
- A fault strength perturbation leads to a quick quasi-static crack propagation followed by a run-away seismic rupture
- The slipping patch outpaces rapidly the fluid front and at nucleation time

$$\frac{a_n}{a_w} \gg \frac{\sqrt{4\alpha t}}{a_w}$$

- The pressurized region is always confined near injection point, i.e.

$$\bar{p}\,(x,t) = \Delta P(t)\delta_{dirac}(x)$$

- GaGe2012 developed semi-analytically an outer and inner asymptotic solutions that are valid at different fault position w.r.t. fluid front location

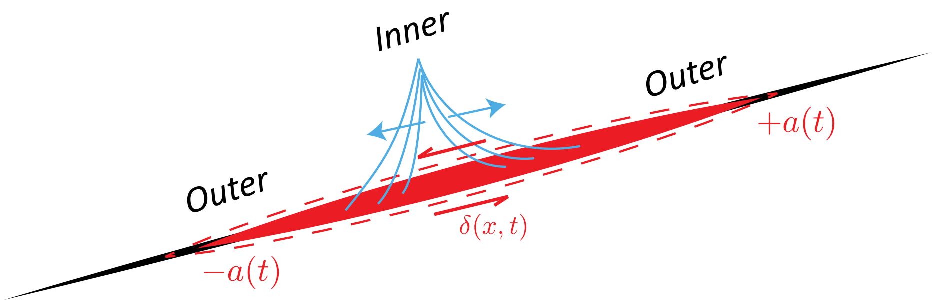

Using the universal outer asymptotic solution:

$$\Delta P(t_n) = \int_{-\infty}^{\infty} \bar{p}\,(x,t_n) \simeq 0.8369\frac{\tau_p - \tau^o}{f_p} a_w$$

By replacing the analytical expression of pore-fluid evolution at nucleation time, we get:

$$\frac{\sqrt{4\alpha t_n}}{a_w} \simeq \left(\frac{2^2 \cdot 0.8369}{\sqrt{\pi}} \cdot \frac{\tau_p - \tau^o}{f_p \Delta P_w} \cdot \frac{t_c}{t_w}\right)^{1/4}$$

$$\Delta P_w = \frac{Q_m a_w \mu}{2k_f\sqrt{\pi} w_h}$$ *Characteristic pore-pressure drop*

Numerical results: unstable fault

$$Q_m/Q^* = 100. \qquad t_c/t_w = 0.5$$

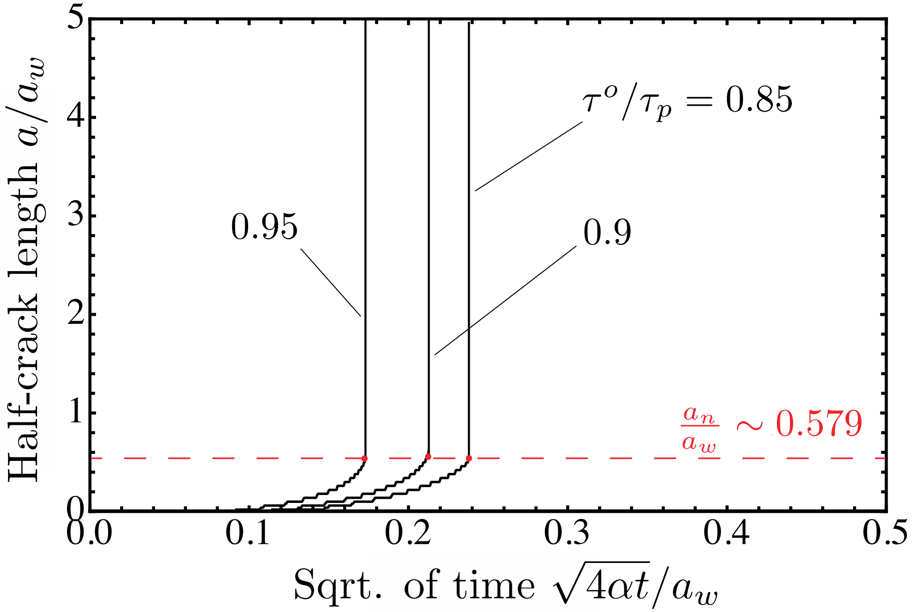

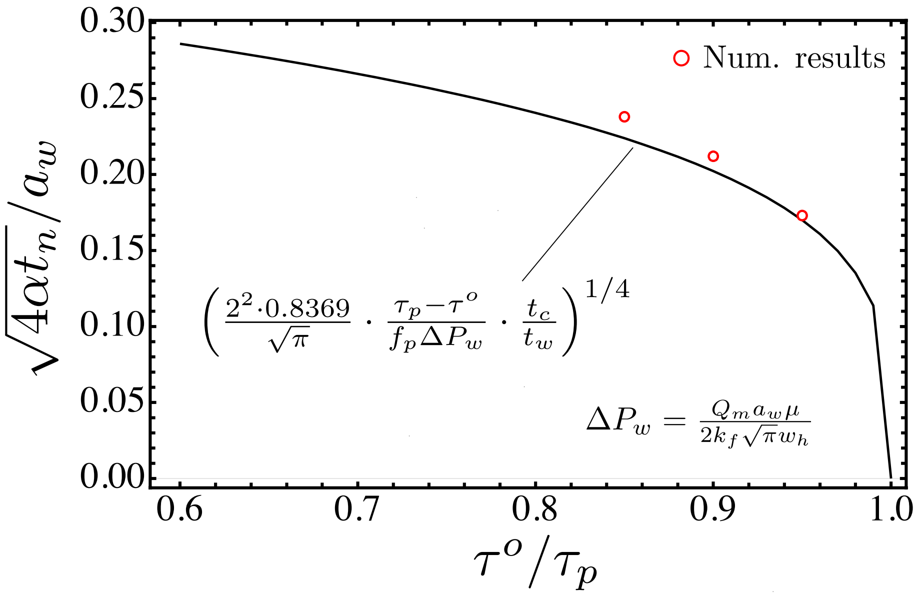

$$f_r/f_p = 0.6$$

Run-away dynamic rupture always present, but its nucleation can be delayed or anticipated!

For a given maximum injection rate, an earlier nucleation with respect to the injection scenario at constant rate only is expected if

$$\frac{t_c}{t_w} < \frac{1}{1.20636^4} \frac{\tau_p - \tau^o}{f_p \Delta P_w}$$

Impact on injection-induced seismicity

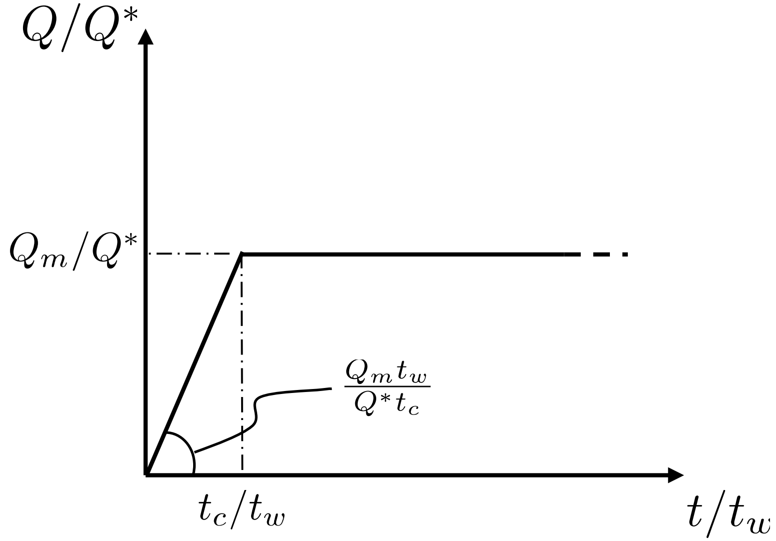

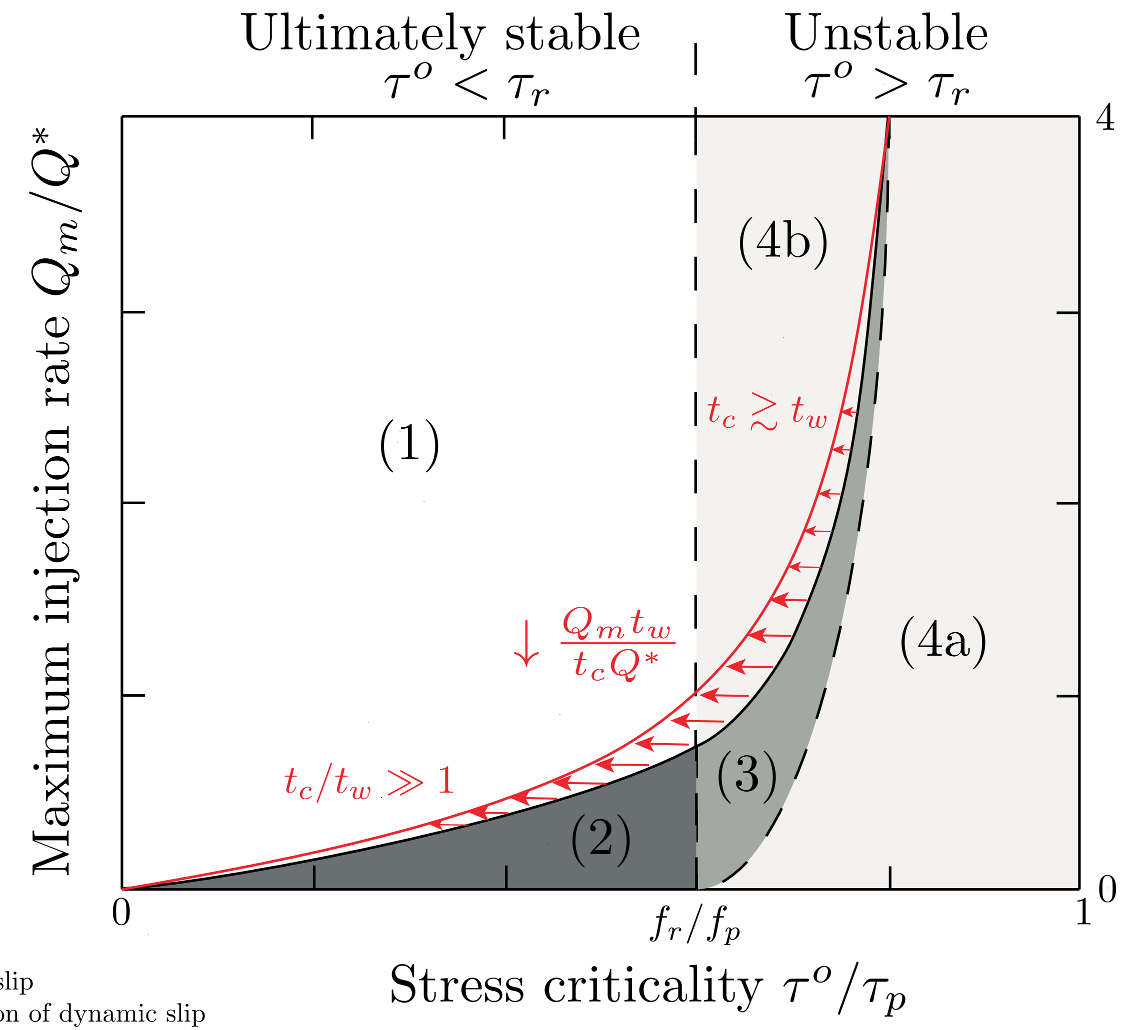

(1) Aseismic slip only
(2) Nucleation and Arrest of dynamic slip
(3) Nucleation, Arrest and re-Nucleation of dynamic slip
(4) Nucleation of dynamic slip

Model limitations

- Neglect of shear-induced dilatancy
  - Ciardo and Lecampion (2019) showed that dilatant hardening effect does impact the transition between aseismic and seismic slip on a pressurized fault due to an undrained pore-pressure drop

$$\Delta p_u = \frac{\Delta w_h}{w_h c_f \sigma'_o}$$

- Neglect of other weakening mechanisms such as flash heating and pore-fluid thermal pressurization (Rice 2006, Viesca & Garagash 2015).
  - Garagash and Germanovich (2021) showed that thermal pressurization increases the dynamic run-out distances on stable faults. However, such an effect is relatively small due to the fact that such a weakening mechanism is expected to occur at a slip scale that is larger than frictional weakening scale δ_w

- Linear-slip weakening friction law
  - It does not allow to investigate scenarios in which fault strength evolve during pressurization, from weakening conditions to strengthening conditions (observed in lab. experiments by Cappa et al. 2019)

Key conclusions

- When the ramp-up time scale is much lower than fluid diffusion time scale, slip propagation on stable faults is driven at constant volumetric rate

- When the ramp-up time scale is much larger than fluid diffusion time scale:
    - Low pressurization rates on stable faults promote a nucleation and arrest of dynamic slip
    - The lower is the pressurization rate applied on stable faults the larger is the dynamic run-out slip distance

- On unstable faults, an initial ramp-up of injection rate may lead to an earlier or later nucleation of run-away rupture, compared to injection case at constant rate.

THANK YOU FOR YOUR ATTENTION!
ANY QUESTIONS?

federico.ciardo@sed.ethz.ch